Review

Influence of Physicochemical Properties of Iron Oxide Nanoparticles on Their Antibacterial Activity

Kishan Nandi Shoudho, Shihab Uddin, Md Mahamudul Hasan Rumon,* and Md Salman Shakil*

ACCESS | Metrics & More | Article Recommendations

ABSTRACT: The increasing occurrence of infectious diseases caused by antimicrobial resistance organisms urged the necessity to develop more potent, selective, and safe antimicrobial agents. The unique magnetic and tunable properties of iron oxide nanoparticles (IONPs) make them a promising candidate for different theragnostic applications, including antimicrobial agents. Though IONPs act as a nonspecific antimicrobial agent, their antimicrobial activities are directly or indirectly linked with their synthesis methods, synthesizing precursors, size, shapes, concentration, and surface modifications. Alteration of these parameters could accelerate or decelerate the production of reactive oxygen species (ROS). An increase in ROS role production disrupts bacterial cell walls, cell membranes, alters major biomolecules (e.g., lipids, proteins, nucleic acids), and affects metabolic processes (e.g., Krebs cycle, fatty acid synthesis, ATP synthesis, glycolysis, and mitophagy). In this review, we will investigate the antibacterial activity of bare and surface-modified IONPs and the influence of physiochemical parameters on their antibacterial activity. Additionally, we will report the potential mechanism of IONPs' action in driving this antimicrobial activity.
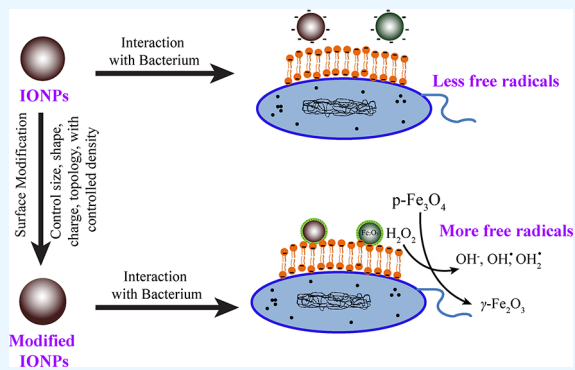
1. INTRODUCTION

Antimicrobial resistance (AMR) is a natural phenomenon in which pathogenic microorganisms develop mechanisms to resist antimicrobial drugs.[1] Due to the severity of AMR, it has become a worldwide concern owing to its correlation with escalated morbidity and mortality. According to the World Health Organization (WHO), AMR has been identified as a global threat to public health, and this era has been reported as the "postantibiotic" era, in which minor infections will be the primary cause of death.[2] According to a study published in 2019, approximately 7.7 million fatalities were ascribed to bacterial infections caused explicitly by antibiotic-resistant bacterial strains.[3] Similarly, a report released in 2022 highlighted that AMR was the primary cause of 1.27 million fatalities and had an indirect role in 4.95 million deaths.[4] Moreover, bacteria develop AMR mechanisms through unsupervised exposure and the wide availability of antibiotics.[5,6] Considering the limited therapeutic options and the severity of AMR, researchers are developing magnetic nanoparticles (MNPs)-based alternative antibacterial agents.[7−9]

Recently, MNPs have received attention in various fields due to their unique magnetic properties, including paramagnetism, tunable magnetism, biocompatibility, drug delivery, and antimicrobial and surface modification properties.[10−16] Like other MNPs, iron oxide nanoparticles (IONPs) are used as magnetic resonance imaging (MRI) contrast dye, biosensors,

diagnosing diseases, drug delivery vehicles, pollutant removal, biomedical machinery, and antimicrobial agents.[17−22] Though divalent metals like iron ions are essential for the growth of microbes, IONPs display nonspecific antibacterial activity by generating electrostatic attraction or repulsion force and reactive oxygen species (ROS).[23−26] Moreover, other parameters could influence the antimicrobial activity of IONPs, including synthesis methods, precursors, size, and concentration.[27] Furthermore, depending on the characteristics of the materials, the physicochemical, electrical, optical, and biological properties of IONPs can be influenced via surface modification. Notably, the coated nanocomplexes exhibit more potent antimicrobial activity than bare IONPs.[28]

Gudkov et al.[29] reported that the antibacterial activity of IONPs could be influenced by altering their synthesis methods and size and discussed several bacteriostatic mechanisms including ROS generation, electrostatic interaction, disruption of the cell membrane, and fragmentation of DNA and protein molecules by inducing free radicals. Moreover, Arias et al.[30]
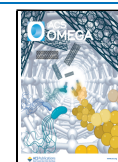
described numerous clinical applications of IONPs (*e.g.,* antimicrobial, anticancer, drug delivery, anticonvulsants, and immunosuppressive agents), toxic effects, and the extent of biocompatibility between IONPs and eukaryotic cells or tissues. Another review addressed the biocompatibility and cytotoxicity of IONPs and how their antibacterial activity was evaluated on a various model organisms using multiple physical and chemical criteria.[31] Alprol et al.[32] highlighted that IONPs synthesized through the green methods are able to exhibit potent antibacterial activity against Gram-positive and moderate inhibition against Gram-negative bacteria by inducing oxidative stress by generating ROS. Furthermore, these authors summarized a few influential parameters associated with the antibacterial efficacy of the IONPs and highlighted their mechanisms against various types of bacteria. Recently, Tasnim et al.[33] discussed the antimicrobial mechanisms and activity of several metal-doped IONPs against a range of bacteria and the potential drawbacks of metal-doped IONPs. Nevertheless, the aforementioned reviews were unable to report the influence of diverse coating materials on the physiochemical properties of IONPs, a comparative analysis of the antibacterial activities of the uncoated and surface-coated IONPs-complexes, their combined mechanistic understanding, and the impact of several parameters like shape, concentration, and precursors on the antibacterial activities of IONPs. Therefore, enlightening the influential parameters of the antibacterial activities of the coated and uncoated IONPs should be weighed up for further research purposes, molecular analysis, and drug development.

In this review, we intend to scrutinize the antimicrobial activities of the uncoated and coated IONPs associated with their physicochemical parameters and their potential mechanisms of action(s). Additionally, we will discuss the antimicrobial efficacy of IONPs concerning their precursors, manufacturing techniques, size, shape, concentration, and surface modification materials.

2. PATHOGENIC BACTERIA

Pathogenic bacteria are microorganisms that induce infectious diseases within the host organism.[34] They exhibit a diverse array of virulence determinants encompassing adherence factors, invasion factors, toxins, capsules, and siderophores, thereby eliciting pathogenicity and instigating disease through host cell invasion and evasion of host defense mechanisms.[35,36]

According to the structural composition of the bacterial cell wall, bacteria can be classified into two distinct categories: Gram-positive and Gram-negative.[37] Several studies have shown that a significant proportion of pathogenic bacteria exhibit Gram-negative characteristics, and due to their distinctive cellular structure, they are more susceptible to antibiotic resistance.[38] Gram-negative bacteria have a complex cellular structure consisting of a peptidoglycan cell wall surrounded by the lipopolysaccharide (LPS) layer. The LPS comprises several virulence factors, including Lipid-A, also known as endotoxin, which is the main virulence factor that causes disease.[39] Gram-negative bacteria release their virulence factor to cause disease during active cellular growth, and after the cell has been lysed, endotoxin is released.[40] Upon releasing these toxins, a robust inflammatory response is initiated within the host organism, potentially resulting in severe and life-threatening symptoms.[41,42] Multiple toxins can potentially inflict diverse harm on the host cell. For instance, producing Shiga toxin by *E. coli* and releasing cholera toxin (CT) by *V.*

cholerae can lead to severe watery diarrhea.[43] The prevailing ailments resulting from pathogenic bacteria include tuberculosis caused by *Mycobacterium tuberculosis,*[44] stomach infections caused by *H. pylori,*[45] and typhoid fever caused by *Salmonella typhi.*[46] More importantly, pathogenic bacteria are able to infiltrate the host's tissue and employ various strategies to exploit the host, potentially resulting in adverse health outcomes and a diverse array of illnesses.[47] Pathogen invasion necessitates a designated point of entry originating from a contaminated source, such as consumable items or inhaling noxious substances. Moreover, pathogens can be transmitted through direct and indirect contact with an infected individual or in poorly ventilated environments.[48]

Pathogenic bacteria pose a significant challenge with the emergence of antibiotic-resistant strains. The overutilization of antibiotics in bacterial populations leads to genetic mutations or the expression of resistance genes, resulting in antibiotic-resistant bacteria development.[49] Resistant genes can be transferred to other bacteria through gene transfer, which may occur through many processes, including conjugation, transmission, and transduction. When pathogenic bacteria develop antibiotic resistance, they become significantly more challenging to treat and present an increased risk to the host organism.[50]

3. IRON OXIDE NANOPARTICLES (IONPs)

Ferromagnetic IONPs find extensive application due to their intricate structure. IONPs exhibit either spinel or inverse spinel crystalline structures, which are determined by the specific type of IONPs and their underlying condition of synthesis.[51] Iron cations and oxide ions are arranged in tetrahedral and octahedral sites.[52,53] However, the positioning of the iron ions is influenced by their oxidation state and structure.[54] Fe^{3+} ions prefer occupying octahedral and tetrahedral sites while maintaining their high spin complex, which arises from their ability to polarize water molecules, leading to the facile cleavage of OH bonds. This phenomenon gives rise to a complex with a reduced charge density and increased stability, accompanied by a smaller ionic radius. In contrast, it was observed that Fe^{2+} exhibits a preference for occupying exclusively octahedral positions within a complex. Moreover, the preferred attributes of the lower charge density and wider ionic radius of Fe^{2+} enable them to maintain a high spin configuration.[55]

IONPs have 14 different types of structures, and 10 of them are found in the Earth's crust due to the abundant existence of oxygen, hydrogen, and iron. Among them, the predominant rock-forming minerals are hematite, magnetite, and goethite. Maghemite, ferrihydrite, and lepidocrocite have a moderate abundance, whereas wustite, bernalite, and feroxyhyte are the least abundant. Hematite (Fe_2O_3) and magnetite (Fe_3O_4) have been extensively studied and applied in different clinical and biomedical domains due to their distinctive attributes such as ferromagnetism, biocompatibility, adjustable magnetic properties, coercivity, high magnetic saturation, magneto-optic performance, anisotropy, magneto-crystalline anisotropy, surface modification properties, and photothermal properties.[56−61] Figure 1 shows the schematical representation of the most abundant IONPs and oxyhydroxides.

There are multiple methodologies for synthesizing IONPs, which can broadly be categorized into two fundamental approaches. The top-down approach involves producing NPs from larger particles.[62] A different approach involves using the
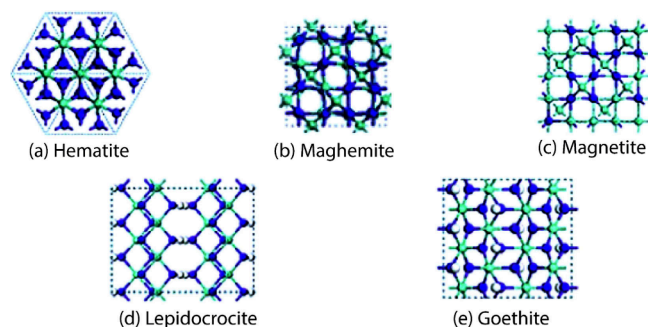
Figure 1. Schematic representation of (a) hematite, (b) maghemite, (c) magnetite, (d) lepidocrocite, and (e) goethite structures. These structures are viewed from the ⟨001⟩ or ⟨0001⟩ directions. The idea of the diagram is taken from Guo and Barnard.[82]

bottom-up method, where NPs are created by utilizing individual molecules and gradually assembling them into the desired nanostructure.[63−65] The methodologies employed in this study encompass coprecipitation (COP), sol−gel (SG), hydrothermal (HDT), one-pot (OP), green synthesis (GRS), sonochemical (SNC), laser pyrolysis (LP), solid-state pyrolytic (SSP), polyol synthesis (PYS), and the microemulsion method (MEL).[17,66−75] Utilizing these synthesis methods significantly influences various characteristics of the IONPs, including their size, cation distribution, magnetic properties,[10] and antimicrobial properties.[76] Moreover, the versatile synthesis process can significantly influence the physicochemical properties of IONPs, which have found widespread applications, including contrast dyes for MRI, specific drug delivery agents, gene carriers for gene therapy, potential antimicrobial agents, potential cancer therapy agents, and biosensors.[77−79] Besides drug delivery, IONPs could enhance the efficacy of Food and Drug Administration (FDA)-approved drugs.[80,81]

4. IONPs AS AN ANTIMICROBIAL AGENT

IONPs possess unique antibacterial properties due to their distinctive physical and chemical attributes, such as their surface charge and ability to generate ROS.[83] The features of IONPs depend on various aspects, such as their synthesis process, precursors, size, shape, and concentration.[9,84]

IONPs could be synthesized using various techniques, including COP, SG, HDT, GRS, LP, MEL, OP, SNC, and PSY methods.[85] Chemically synthesized methods necessitate the use of intense radiation and result in the production of very hazardous residues. The GRS method requires minimal precursors and energy for initiation, with plant extracts as the reducing agent. Interestingly, the plant extracts possess inherent therapeutic characteristics that contribute to their notable antibacterial efficacy.[85,86] Moreover, various iron precursors utilized in the synthesis procedures may influence the properties of IONPs (Table 1). Hence, precursors and synthesis methods are considered crucial parameters that influence the antibacterial activity of IONPs.

The antimicrobial efficacy of IONPs also varies by size, which influences the surface area-to-volume ratio. The small size of the IONPs indicates a larger surface area to volume ratio; consequently, the increased surface area would allow IONPs to cover a more significant portion of the bacteria, resulting in more frequent interactions with the bacterial cell membrane and causing damage through electrostatic attraction and repulsion force.[104−106] The antibacterial effectiveness of

the IONPs also depends on the bacterial strains due to their differences in cell wall structure. The Gram-positive bacteria have a thick peptidoglycan layer consisting of a net negative charge due to teichoic acid.[107] On the contrary, Gram-negative bacteria consist of a thin peptidoglycan layer and an overlaid lipopolysaccharide layer, which has an elevated net negative charge. IONPs interact with the negatively charged bacterial cell membrane through an electrostatic force that induces depolarization and disrupts the integrity of the cell membrane.[103,108,109] Hence, due to the structural difference in the cellular composition, Gram-positive bacteria are more susceptible to IONPs than Gram-negative bacteria. Moreover, IONPs implicate nonspecific mechanistic behavior to eradicate pathogenic bacteria, such as inducing oxidative stress by producing ROS.[110−112] These have the ability to inhibit the function of DNA, proteins, and enzymes, leading to bacterial cell death.[76,113] IONPs do not adhere to a single strategy for inhibiting bacteria. As a result, bacteria struggle to develop resistance mechanisms against them.[114]

5. PARAMETERS INFLUENCING ANTIMICROBIAL ACTIVITY

5.1. Synthesis. *5.1.1. COP Method.* COP is the most common, economical, and versatile method for generating IONPs. This method generates IONPs under alkaline conditions through precipitation in a nonoxidizing environment where Fe^{2+}/Fe^{3+} salt precursors are mixed in a 1:2 ratio.[96,115−117] Moreover, the COP technique can effectively influence the size and morphology of the IONPs by altering some variables during synthesis, including the ionic strength, pH, temperature, concentration, and ratio of the precursors.[118]

IONPs synthesized via the COP method exhibited notable antibacterial activity against bacteria; for instance, the bare Fe_3O_4 exhibited moderate antibacterial activity against *E. coli, P. mirabilis*, and *B. subtilis.*[96] However, the antibacterial activity can be increased through surface modification of IONPs. Recently, Sharaf et al.[87] reported that IONPs generated and modified using COP procedures showed notable antibacterial efficacy against several *E. coli* and *S. aureus.* An inhibitory zone ranging from 9 to 12 mm was detected against both bacteria when the Fe_3O_4 was coated with RHL. Interestingly, surface modification of the IONPs using RHL, PVA, GA, and p-CoA caused a 4-fold increase in zone of inhibition (ZOI). Conversely, the Fe_2O_3 generated by COP without other substances demonstrated an enhanced antibacterial effect compared to magnetite. It displayed a ZOI ranging from 11 to 21 mm against *B. cereus, S. aureus, E. coli*, and *S. typhi* at greater concentrations.[59] Compared to bare Fe_3O_4 NPs, the Fe_2O_3 NPs showed pronounced bacteriostatic action against *E. coli* and *S. aureus,*[59,98] while a study by Abdulsada et al.[93] displayed that IONPs synthesized and modified with poly-(ethylene glycol) (PEG) and gentamicin (GEN) through COP had an elevated antibacterial activity compared to the bare IONPs. Despite having the same synthesis method, IONPs exhibit a varying response against identical bacteria, and several factors may contribute to this variation, including precursors, shape, size, and coating material. Thus, IONPs synthesized by the COP method exhibited remarkable antimicrobial properties.[99]

5.1.2. SG Method. The SG method is a bottom-up synthesis method where irreversible chemical reactions occur. Certain chemical interactions, including hydrolysis and condensation, form a sol and a three-dimensional polymeric structure termed

Table 1. Antimicrobial activity and potential mechanism of chemically synthesized IONPs[a]

NPs	Particle size (nm)	Shape	Precursor	Synthesis method	Coating Material	Con. (μg/mL)	Organism	ZOI (mm)	MIC (μg/mL)	MBC (μg/mL)	ICS50 (μg/mL)	Mechanism	ref.
Fe₃O₄	~254	Spherical	FeCl₃·6H₂O, FeCl₂·4H₂O, NaOH, DW & HCl	COP	RHL	NR	Escherichia coli (O157: H7)	~9	64	128	NR	The RHL coated-Fe₃O₄@PVA@p-CoA/GA biosurfactant mediated the structural and confirmational changes on the cell surface. Moreover, the coating material intercalated with the DNA, inhibited the replication, transcription and translation process by generating ROS. The ROS induced oxidative stress that led to apoptosis of bacterial cells.	87
					RHL, PVA, GA, p-CoA	NR	Escherichia coli (O26: H11)	~10	4	8			
							Escherichia coli (O78: H10)	~12	32	64			
							Staphylococcus aureus (MSSA)	~12	16	32			
							Staphylococcus aureus (MRSA)	~10	32	64			
							Staphylococcus aureus (VRSA)	~8	64	128			
							Escherichia coli (O157: H7)	35	32	64			
							Escherichia coli (O26: H11)	45	1	2			
							Escherichia coli (O78: H10)	40	16	32			
							MSSA	40	4	8			
							MRSA	30	16	32			
							VRSA	25	32	64			
Fe₂O₃	36.1	Spherical	FeCl₃·6H₂O, TiCl₄·2H₂O, CTAB & NaOH	COP	PR	5000	Bacillus subtilis	13	NR	NR	NR	The Fe₂O₃ and TiO₂ polyester nanocomposite enhanced the interaction with bacterial cell membranes. It created an ionic imbalance in the bacterial cell, resulting in cell apoptosis.	88
							Staphylococcus aureus	18					
							Escherichia coli	13					
							Pseudomonas aeruginosa	12					
							Candida albicans	29					
							Aspergillus niger	26					
Fe₃O₄	48	Spherical	FeSO₄, FeCl₃, DW, NH₄OH & HNO₃	COP	RHL	NR	Pseudomonas aeruginosa	NR	1000	NR	NR	Fe₃O₄ induced oxidative stress in the bacterial cell by producing ROS which caused cell death. Again, the Rhamnolipid-coated Fe₃O₄ interacted with extracel-	89

Table 1. continued

NPs	Particle size (nm)	Shape	Precursor	Synthesis method	Coating Material	Con. (µg/mL)	Organism	ZOI (mm)	MIC (µg/mL)	MBC (µg/mL)	ICS0 (µg/mL)	Mechanism	ref.
							Staphylococcus aureus	NR	1000	NR		lular polymeric substances (EPS), which could affect the hydrophobicity of bacterial cell surface and hinder biofilm generation.	
IO QDNPs	<80	Spherical	Fe (NO$_3$)$_3$·9H$_2$O, argon gas, DW, ethanol & NaOH	COP and HDT.	NR	NR	Escherichia coli PTCC 1330	NR	1	NR	NR	The IO-QDNPs changed membrane potential and damaged the biological mechanism by interacting with the cell membranes and subunit of the ribosome. Again, ROS-mediated structural and confirmational changes in DNA were responsible for bacterial cell death.	90
							Staphylococcus aureus PTCC 1053	NR	0.5				
							Serratia marcescens PTCC1621	NR	0.5				
							Pseudomonas aeruginosa PTCC1074	NR	0.5				
							Staphylococcus aureus PTCC. 1112	NR	1				
							Micrococcus luteus PTCC. 1110	NR	4				
							Bacillus subtilis PTCC. 1023	NR	0.5				
							Staphylococcus epidermidis PTCC 1114	NR	0.5				
Fe$_3$O$_4$	~39.56	Spherical	FeCl$_2$·4H$_2$O, FeCl$_3$·6H$_2$O & NH$_4$OH	COP	TiO$_2$	NR	Escherichia coli	NR	150	NR	NR	TiO$_2$-coated IONPs had potent toxicity against bacterial cells, so they exhibited antibacterial activity when they interacted with the cell membranes.	91
							Klebsiella pneumonia	NR	150				
							Bacillus subtilis	NR	150				
							Staphylococcus aureus	NR	150				
							Escherichia coli	NR	150				
							Klebsiella pneumonia	NR	150				
							Bacillus subtilis	NR	150				

Table 1. continued

NPs	Particle size (nm)	Shape	Precursor	Synthesis method	Coating Material	Con. (μg/mL)	Organism	ZOI (mm)	MIC (μg/mL)	MBC (μg/mL)	ICS0 (μg/mL)	Mechanism	ref.
SPION	23.32 ± 1.17	NR	Iron salt and dimer-captosuccinic acid	Two-step COP process.	NR	NR	Staphylococcus aureus	NR	150	NR	NR	SPION mediated the conformational and structural changes on the cell surface and disrupted the cell membrane.	92
							MARS	NR	530.796 ± 15.241	NR			
									495.993 ± 3.909	NR			
									581.353 ± 10.26	NR			
									457.871 ± 21.064	NR			
Fe$_3$O$_4$	31.09	Spherical	FeCl$_2$;2H$_2$O, FeCl$_3$;6H$_2$O, N$_2$, DW & NH$_4$OH.	COP	NR	NR	Staphylococcus epidermidis	17.33 ± 0.57	25	50	NR	Generally, photolytic generation of ROS induces oxidative stress in the cell. Also, due to the vibration of magnetic fields, IONPs lead bacterial cells to death.	93
							Proteus mirabilis	17.51 ± 0.57	50	100			
							Acinetobacter baumannii	17.66 ± 0.57	50	100			
					PEG	NR	Staphylococcus epidermidis	19.66 ± 0.57	25	50			
							Proteus mirabilis	21.66 ± 0.57	50	100			
							Acinetobacter baumannii	22.00 ± 0.46	50	100			
					GEN	NR	Staphylococcus epidermidis	21.33 ± 1.15	50	100			
							Proteus mirabilis	23.66 ± 0.57	25	50			
							Acinetobacter baumannii	23.66 ± 0.57	50	100			
					PEG+ GEN	NR	Staphylococcus epidermidis	23.66 ± 0.057	50	100			
							Proteus mirabilis	25.66 ± 0.57	25	50			
							Acinetobacter baumannii	26.33 ± 0.57	50	100			
Fe$_2$O$_3$	14.2 ± 0.5	Spherical	FeCl$_2$;4H$_2$O, FeCl$_3$;6H$_2$O, DW, NH$_4$OH, HNO$_3$ HCl & Fe (NO$_3$)$_3$;9H$_2$O	COP	Teicoplanin	NR	Bacillus subtilis (ATCC 6633)	NR	2	>128	NR	Fe$_2$O$_3$ NPs induced ROS, which induced oxidative stress and led to programmed cell death as well as autophagic activity.	94
							Staphylococcus aureus (ATCC 6538Pb (MSSA))	NR	2	128			
							Staphylococcus aureus (ATCC 43300 (MRSA))	NR	2	>128			
							Enterococcus, faecalis (ATCC 29212)	NR	1	32			

Table 1. continued

NPs	Particle size (nm)	Shape	Precursor	Synthesis method	Coating Material	Con. (μg/mL)	Organism	ZOI (mm)	MIC (μg/mL)	MBC (μg/mL)	ICS50 (μg/mL)	Mechanism	ref.
							Enterococcus faecalis (ATCC 51299 (VanB))	NR	2	>128			
							Enterococcus faecalis (9160188401-EF-34 (VanA))	NR	>128	>128			
							Escherichia coli (ATCC 35218)	NR	>128	>128			
Fe$_2$O$_3$	25.34	Hexagonal	FeSO$_4$·7H$_2$O, Co(NO$_3$)$_2$·6H$_2$O, NaOH & DW	COP	NR	400	Bacillus subtilis	11	Escherichia coli			Fe$_2$O$_3$ NPs induced ROS, which triggered oxidative stress and led to cell death.	59
							Staphylococcus aureus	12	900	NR			
							Escherichia coli	19					
							Salmonella typhi	12					
						600	Bacillus subtilis	15					
							Staphylococcus aureus	13					
							Escherichia coli	20					
							Salmonella typhi	13					
						800	Bacillus subtilis	17					
							Staphylococcus aureus	15					
							Escherichia coli	21					
							Salmonella typhi	16					
Fe$_3$O$_4$	10.64 ± 4.73	Spherical	FeSO$_4$·7H$_2$O, FeCl$_3$·6H$_2$O, DW & NaOH	COP	Oleic acid	NR	Escherichia coli	NR	NR	NR	NR	The antibacterial activity of Fe$_3$O$_4$ NPs was mediated by electrostatic interaction between NPs and the cell membranes. Also, the ROS played a vital role in cell apoptosis.	95
							Enterococcus hirae	NR					
Fe$_3$O$_4$	10–30	Spherical	NR	COP	NR	12.5	Escherichia coli	7	NR	NR	NR	Fe$_3$O$_4$ mediated antibacterial activity by causing damaged to the proteins and DNA in the bacterial cell by generating ROS.	96
							Proteus mirabilis	7					
							Bacillus subtilis	7					
						25	Escherichia coli	7					
							Proteus mirabilis	7					
							Bacillus subtilis	7					
						50	Escherichia coli	8					
							Proteus mirabilis	8					
							Bacillus subtilis	8					

Table 1. continued

NPs	Particle size (nm)	Shape	Precursor	Synthesis method	Coating Material	Con. (μg/mL)	Organism	ZOI (mm)	MIC (μg/mL)	MBC (μg/mL)	IC50 (μg/mL)	Mechanism	ref.
						Fe₃O₄ + Plant extract							
						12.5	Escherichia coli	11	NR	NR	NR		
							Proteus mirabilis	16					
							Bacillus subtilis	7					
						25	Escherichia coli	12					
							Proteus mirabilis	17					
							Bacillus subtilis	8					
						50	Escherichia coli	13					
							Proteus mirabilis	18					
							Bacillus subtilis	10					
Fe₃O₄	6–9	Spherical	FeCl₃, FeSO₄, DW, NH₄OH, PEG & ethyl alcohol	COP	NR	NR	Serratia marcescens	NR	32	NR	NR	ROS produced by IONPs moderated physical damage or chemical damage by interacting with the cell membranes, leading to bacterial cell death.	97
							Escherichia coli	NR	64				
							Pseudomonas aeruginosa	NR	128				
							Listeria monocytogenes	NR	32				
Fe₃O₄	24	NR	FeCl₃, FeCl₂, DW, Argon gas & NaOH	COP	NR	40	Bacillus cereus	13	5	80	NR	IONPs could interact with DNA and proteins and mediate their conformational changes.	66
							Klebsiella pneumoniae	15					
						80	Bacillus cereus	22					
							Klebsiella pneumoniae	26					
Fe₃O₄	10–14	Spherical	FeCl₃, FeCl₂, DW, & NaOH	COP	NR	500	Staphylococcus aureus	<10	Staphylococcus aureus	NR	NR	The IONPs damaged the cell membrane by inducing ROS. When IONPs are conjugated with gentamicin, bacterial growth is constrained by both mechanisms. By inhibiting the protein synthesis and damaging the cell membrane.	98
							Escherichia coli	<10					
							Bacillus subtilis	<10					
							Pseudomonas aeruginosa	<10	25,000	30,000			
						1000	Staphylococcus aureus	<10	Escherichia coli		NR		
							Escherichia coli	<10	28,000	35,000			
							Bacillus subtilis	<10					
							Pseudomonas aeruginosa	<10					

Table 1. continued

NPs	Particle size (nm)	Shape	Precursor	Synthesis method	Coating Material	Con. (μg/mL)	Organism	ZOI (mm)	MIC (μg/mL)	MBC (μg/mL)	ICS0 (μg/mL)	Mechanism	ref.
						3000	Staphylococcus aureus	<10	Bacillus subtills		NR		
							Escherichia coli	<10	20,000	25,000			
							Bacillus subtills	<10					
							Pseudomonas aeruginosa	<10					
						5000	Staphylococcus aureus	<10	Pseudomonas aeruginosa		NR		
							Escherichia coli	<10	30,000	35,000			
							Bacillus subtills	<10					
							Pseudomonas aeruginosa	<10					
					GEN	500	Staphylococcus aureus	<10	Staphylococcus aureus		NR		
							Escherichia coli	<10	2000	3000			
							Bacillus subtills	12.5					
							Pseudomonas aeruginosa	<10					
						1000	Staphylococcus aureus	10	Escherichia coli		NR		
							Escherichia coli	<10	2500	3000			
							Bacillus subtills	13					
							Pseudomonas aeruginosa	<10					
						3000	Staphylococcus aureus	13	Bacillus subtills		NR		
							Escherichia coli	<10	1500	2500			
							Bacillus subtills	25					
							Pseudomonas aeruginosa	<10					
						5000	Staphylococcus aureus	16	Pseudomonas aeruginosa		NR		
							Escherichia coli	11	3000	4000			
							Bacillus subtills	33					
							Pseudomonas aeruginosa	<10					
Fe₃O₄	~100	Spherical	Oleic amine, ethylene glycol, FeCl₃·6H₂O, & sodium acetate	HDT	NR	200	Klebsiella pneumoniae	22 ± 1.0	Klebsiella pneumoniae		NR	IONPs generate ROS molecules that interact with the ion transportation channel and the DNA and induce oxidative stress to eliminate bacterial cells.	68
							Staphylococcus aureus	28 ± 0.5	50	100			
							Enterococcus faecalis	25 ± 0.0					
							Pseudomonas aureginosa	18 ± 1.0					

Table 1. continued

NPs	Particle size (nm)	Shape	Precursor	Synthesis method	Coating Material	Con. (µg/mL)	Organism	ZOI (mm)	MIC (µg/mL)	MBC (µg/mL)	IC50 (µg/mL)	Mechanism	ref.
Fe_3O_4	35	Spherical	Fe $(NO_3)_3 \cdot 9H_2O$, DW, & NH_3	CC	NR	100	Klebsiella pneumoniae	20. ± 0.0	Staphylococcus aureus				99
							Staphylococcus aureus	25 ± 0.0	6.25	12.5			
							Enterococcus faecalis	20 ± 1.0					
							Pseudomonas aureginosa	16 ± 0.0					
						50	Klebsiella pneumoniae	18 ± 1.0	Enterococcus faecalis				
							Staphylococcus aureus	22 ± 2.0	6.25	12.5			
							Enterococcus faecalis	17 ± 0.5					
							Pseudomonas aureginosa	15 ± 0.5					
						25	Klebsiella pneumoniae	15 ± 0	Pseudomonas aureginosa				
							Staphylococcus aureus	20 ± 1.0	50	50			
							Enterococcus faecalis	11 ± 0.0					
							Pseudomonas aureginosa	12 ± 0.0					
						25	Escherichia coli	15	NR	NR	NR	Fe_3O_4 generated ROS that disrupted membrane protein and penetrated the bacterial membrane. It induced oxidative stress, which led to cell death.	
							Proteus vulgaris	11					
							Staphylococcus aureus	9					
							Xanthomonas	10					
						30	Escherichia coli	16					
							Proteus vulgaris	12					
							Staphylococcus aureus	12					
							Xanthomonas	12					
						40	Escherichia coli	17					
							Proteus vulgaris	15					
							Staphylococcus aureus	14					
							Xanthomonas	14					
						50	Escherichia coli	17					
							Proteus vulgaris	20					
							Staphylococcus aureus	15					
							Xanthomonas	15					

Table 1. continued

NPs	Particle size (nm)	Shape	Precursor	Synthesis method	Coating Material	Con. (µg/mL)	Organism	ZOI (mm)	MIC (µg/mL)	MBC (µg/mL)	ICS50 (µg/mL)	Mechanism	ref.
IO	14–23	Hexagonal	$FeSO_4 \cdot 7H_2O$, β-Cyclodextrin, N_2, & sodium borohydride	CS	Beta-cyclodextrin	60	Escherichia coli	15				IONPs interacted with the cell wall and facilitated cell permeability, hindering cellular activity and resulting in the disruption of bacterial cells.	100
							Proteus vulgaris	20					
							Staphylococcus aureus	11					
							Xanthomonas	8					
						80	Escherichia coli	15					
							Proteus vulgaris	12					
							Staphylococcus aureus	12					
							Xanthomonas	14					
						100	Escherichia coli	21					
							Proteus vulgaris	21					
							Staphylococcus aureus	15					
							Xanthomonas	15					
						NR	Staphylococcus aureus	43.83 ± 0.75	100	NR	NR		
							Klebsiella pneumonia	39.83 ± 1.33	300				
							Salmonella typhi	20 ± 0.63	200				
Fe₃O₄	~25	NR	$Fe(NO_3)_3$, DW, Ethylene glycol.	SG	NR	5	Bacillus spp.	23	NR	NR	NR	The addition of citric acid increased the ROS generation and the electro-hole pair generation, leading to the decay of the bacterial surface.	101
						10	Escherichia coli	19					
							Bacillus spp.	25					
						15	Escherichia coli	20					
							Bacillus spp.	26					
						20	Escherichia coli	21					
							Bacillus spp.	27					
							Escherichia coli	22					
					Citric acid	5	Bacillus spp.	32					
							Escherichia coli	29					
						10	Bacillus spp.	31					
							Escherichia coli	22					
						15	Bacillus spp.	33					
							Escherichia coli	23					
						20	Bacillus spp.	36					
							Escherichia coli	26					
Fe₃O₄	NR	NR	$Fe(NO_3)_3 \cdot 9H_2O$, ethanol	SG	NR	50	Enterobacter aerogenes	NR	NR	NR	NR	Fe^{3+} ions interact with the negatively charged membrane, decreasing the membrane integrity.	102

Table 1. continued

NPs	Particle size (nm)	Shape	Precursor	Synthesis method	Coating Material	Con. (µg/mL)	Organism	ZOI (mm)	MIC (µg/mL)	MBC (µg/mL)	IC50 (µg/mL)	Mechanism	ref.
						100						By entering the cell, IONPs produce ROS, which disrupts the cell organelles and eradicates the cell.	
						150	Staphylococcus aureus						
						200							
Fe$_2$O$_3$	50−110	Spherical	SDS, DMF & iron pressed pellet.	PLA	NR	Fe$_2$O$_3$ + DMF						The electrons in the photocatalytic process were absorbed by free radicals and produced OH$^-$ radicals. These radicals inhibited the growth of bacteria by induced oxidative stress generated by ROS.	103
						4250 (20 mJ)	Escherichia coli	19	NR	NR	NR		
							Pseudomonas aeruginosa	17					
							Serritia marcescens	20					
							Staphylococcus aureus	21					
						4250 (40 mJ)	Escherichia coli	22					
							Pseudomonas aeruginosa	16					
							Serritia marcescens	24					
							Staphylococcus aureus	18					
						4250 (60 mJ)	Escherichia coli	18					
							Pseudomonas aeruginosa	27					
							Serritia marcescens	17					
							Staphylococcus aureus	22					
						4250 (80 mJ)	Escherichia coli	17					
							Pseudomonas aeruginosa	27					
							Serritia marcescens	20					
							Staphylococcus aureus	23					
						Fe$_2$O$_3$ + SDS							

Table 1. continued

NPs	Particle size (nm)	Shape	Precursor	Synthesis method	Coating Material	Con. (μg/mL)	Organism	ZOI (mm)	MIC (μg/mL)	MBC (μg/mL)	IC50 (μg/mL)	Mechanism	ref.
						4250 (20 mJ)	Escherichia coli	25					
							Pseudomonas aeruginosa	13					
							Serritia marcescens	27					
							Staphylococcus aureus	30					
						4250 (40 mJ)	Escherichia coli	27					
							Pseudomonas aeruginosa	27					
							Serritia marcescens	30					
							Staphylococcus aureus	35					
						4250 (60 mJ)	Escherichia coli	23					
							Pseudomonas aeruginosa	22					
							Serritia marcescens	15					
							Staphylococcus aureus	28					
						4250 (80 mJ)	Escherichia coli	20					
							Pseudomonas aeruginosa	19					
							Serritia marcescens	18					
							Staphylococcus aureus	30					

[a]NPs: Nanoparticles; Con.: Concentration; ZOI: zone of inhibition; ref: References; ROS: Reactive oxygen species; NR: Not reported; MIC: Minimum inhibitory concentration; MBC: Minimum bactericidal concentration; IC$_{50}$: Half maximal inhibitory concentration; COP: Coprecipitation; HDT: Hydrothermal; CS: Chemical synthesis; SG: Sol–gel; TDP: Thermal decomposition; PLA: Pulsed laser ablation; FeCl$_3$·6H$_2$O: Ferric chloride hexahydrate; FeCl$_2$·4H$_2$O: Ferrous chloride tetrahydrate; FeSO$_4$: Ferrous sulfate; TiCl$_4$·2H$_2$O: Titanium tetrachloride; FeSO$_4$·7H$_2$O: Ferrous sulfate; Fe (NO$_3$)$_3$·9H$_2$O: Ferric nitrate nonahydrate; DW: Deionized water; CTAB: Trimethylammonium bromide; PR: polyester resin; RHL: Rhamnolipid; DMF: Dimethylformamide; GEN: Gentamicin; kan: Kanamycin; CC: Chemical combustion; PEG: Poly(ethylene glycol); IO: Iron oxide; QNDPs: Quantum dots nanoparticles; SPION: Superparamagnetic Iron oxide nanoparticles; PVA: Poly(vinyl alcohol) polymer; GA: Gallic acid; p-CoA: p-Coumaric acid; RHL coated-Fe$_3$O$_4$@PVA@p-CoA/GA: Rhamnolipid coated Iron oxide with Poly(vinyl alcohol) polymer; Gallic acid & p-Coumaric acid; MSSA: Methicillin-sensitive Staphylococcus aureus; MRSA: Methicillin-resistant Staphylococcus aureus; VRSA: Vancomycin-resistant Staphylococcus aureus.

Table 2. Antimicrobial activity and potential mechanism of Green synthesized IONPs[a]

NPs	Particle size (nm)	Shape	Precursor	Synthesis method	Coating Material	Con. (μg/mL)	Organism	ZOI (mm)	MIC (μg/mL)	MBC (μg/mL)	IC50 (μg/mL)	Mechanism	ref
α-Fe$_2$O$_3$	28.17	Spherical	FeCl$_3$·6H$_2$O, & Capparis zeylanica leaf extract	GRS	NR	25	Staphylococcus aureus	23 ± 2.23	NR	NR	15.6	Fe$_2$O$_3$ eliminates bacterial cells by inducing oxidative stress by generating ROS molecules.	140
							Streptococcus pyogenes	25 ± 2.56					
							Escherichia coli	23 ± 1.34					
							Pseudomonas aeruginosa	22 ± 1.23					
							Candida albicans	19 ± 0.98					
							Aspergillus niger	17 ± 1.62					
Fe$_2$O$_3$	13.13–24.93	Hexagonal	Purpureocillium lilacinum, & FeSO$_4$	GRS	NR	NR	Staphylococcus aureus	26.5	NR	NR	NR	Fe$_2$O$_3$ mediated structural or conformational change of DNA, which disrupted enzymatic activity by generating hydroxyl free radicals. Additionally, Fe$_2$O$_3$ induced oxidative stress, leading to apoptosis of bacterial cells.	131
							Bacillus subtilis	24.8					
							Escherichia coli	19.5					
							Pseudomonas aeruginosa	17					
IO	3.31–10.69	Spherical	FeCl$_3$ & Penicillium spp.	GRS	NR	250	Staphylococcus aureus	12 ± 0.6	NR	NR	NR	IONPs diffuse into the intercellular membrane and damage DNA and protein and decompose the lipopolysaccharide layer by generating ROS, which induces oxidative stress. Hence, bacterial growth was inhibited.	139
							Escherichia coli	11.3 ± 1.2					
							Klebsiella pneumoniae	11.3 ± 0.6					
							Shigella sonnie	11.3 ± 0.6					
							Pseudomonas aureginosa	11.3 ± 0.6					
Fe$_2$O$_3$	40	Spherical	Citrus leaf extract, DW, & FeCl$_3$	GRS	NR	100	Bacillus subtilis	26.1 ± 0.24	NR	NR	NR	Fe$_2$O$_3$ disrupted the enzymatic activity by interacting with cell surface proteins and the biological metabolites, resulting in bacterial cell apoptosis.	69
							Klebsiella pneumoniae	21.5 ± 0.36					
						50	Bacillus subtilis	24.1 ± 0.37					
							Klebsiella pneumoniae	18.3 ± 0.49					
						25	Bacillus subtilis	12.8 ± 0.69					
							Klebsiella pneumoniae	11.7 ± 0.53					
Fe$_2$O$_3$	5–100	Spherical	FeCl$_3$, Tamarix Aphylla extract & NaOH	'GRS	NR	1000	Escherichia coli	11	30 ± 0.5	NR	NR	Fe$_2$O$_3$ diffused into the cytoplasmic space, disrupted the enzymatic activity, damaged the DNA and led to death.	141
							Bacillus subtilis	12	30 ± 0.5				

Table 2. continued

NPs	Particle size (nm)	Shape	Precursor	Synthesis method	Coating Material	Con. (μg/mL)	Organism	ZOI (mm)	MIC (μg/mL)	MBC (μg/mL)	IC50 (μg/mL)	Mechanism	ref
FeO	93.9	Spherical	FeSO$_4$·7H$_2$O Thymbra spicata leaf extract & ethyl alcohol.	GRS	NR		Bacillus cereus	NR	200	200	NR	The free radical generated by FeO NPs interacted with the cellular membrane, which induced oxidative stress and caused cell apoptosis.	142
							Staphylococcus aureus		>200	>200			
							Escherichia coli		>200	>200			
							Salmonella typhimurium		100	200			
					NR		Bacillus cereus	NR	200	>200	NR		
							Staphylococcus aureus		>200	>200			
							Escherichia coli		>200	>200			
							Salmonella typhimurium		200	>200			
IONPs	150–200	Spherical	FeSO$_4$·7H$_2$O, Lawsonia inermis extract, NaOH, DW & methanol.	GRS	L-tyr	40	Staphylococcus aureus	16	NR	NR	NR	L-tyrosine-coated IONPs interacted with the lipid bilayer, disrupting the bacterial cell membrane and leading to cell apoptosis.	143
							Staphylococcus tryphimurium	15					
FeO	82 ± 7.0	Spherical	FeCl$_3$, PMC, & DW	GRS	NR	10	Escherichia coli	20	NR	NR	NR	FeO-NPs interacted with the bacteria's thiol group, which induced oxidative stress and caused cell death.	144
							Salmonella typhi	24					
							Staphylococcus aureus	26					
							Shigella	24					
							Pasteurella multocida	18					
							Pseudomonas aeruginosa	16					
FeO	10–25	Spherical	FeCl$_3$ & GMAM	GRS	NR	NR	Escherichia coli	NR	NR	200	NR	FeO-NPs interacted with bacterial cell membranes and induced oxidative stress by producing ROS, leading to cell death.	145
							Pseudomonas aeruginosa	NR	NR	200			
							Staphylococcus aureus	NR	NR	200			
Fe$_3$O$_4$	84.81	NR	FeCl$_2$, FeCl$_3$, DW, MH, CCP, & NaOH	GRS	Kan	25 μg (NPs) + 5 μg (antibiotic)	Bacillus cereus (ATCC 13601)	10.35 ± 0.17				Antibiotics or anticandidal-coated Fe$_3$O$_4$ adheres to the cell surface via electromagnetic attractions; they interact with the thiol group which induces oxidative stress and leads to microbial cell apoptosis.	123
							Escherichia coli (ATCC 43890)	18.44 ± 0.41					
							Listeria monocytogenes (ATCC 19115)	16.00 ± 0.86					

Table 2. continued

NPs	Particle size (nm)	Shape	Precursor	Synthesis method	Coating Material	Con. (μg/mL)	Organism	ZOI (mm)	MIC (μg/mL)	MBC (μg/mL)	IC50 (μg/mL)	Mechanism	ref
							Staphylococcus aureus (ATCC 49444)	13.09 ± 0.30					
							Salmonella typhimurium (ATCC 43174)	13.17 ± 0.26					
				Rif	25 μg (NPs) + 5 μg (antibiotic)		Bacillus cereus (ATCC 13601)	9.36 ± 0.28					
							Escherichia coli (ATCC 43890)	9.62 ± 0.51					
							Listeria monocytogenes (ATCC 19115)	0					
							Staphylococcus aureus (ATCC 49444)	21.99 ± 1.32					
							Salmonella typhimurium (ATCC 43174)	0					
				Amp	25 μg (NPs) + 5 μg (antibiotic)		Candida albicans (KACC 30003)	10.63 ± 0.55					
							Candida albicans (KACC 30062)	17.68 ± 0.52					
							Candida glabrata (KBNO6P00368)	10.11 ± 0.20					
							Candida glochares (KACC 30061)	17.35 ± 0.35					
							Candida saitoana (KACC 41238)	12.30 ± 0.54					
	48.91			GRS	Kan	25 μg (NPs) + 5 μg (antibiotic)	Bacillus cereus (ATCC 13601)	10.04 ± 0.41					
							Escherichia coli (ATCC 43890)	19.65 ± 0.60					
							Listeria monocytogenes (ATCC 19115)	13.10 ± 0.34					
							Staphylococcus aureus (ATCC 49444)	12.28 ± 0.15					
							Salmonella typhimurium (ATCC 43174)	12.42 ± 0.28					
				Rif	25 μg (NPs) + 5 μg (antibiotic)		Bacillus cereus (ATCC 13601)	10.66 ± 0.16					
							Escherichia coli (ATCC 43890)	9.29 ± 0.57					

Table 2. continued

NPs	Particle size (nm)	Shape	Precursor	Synthesis method	Coating Material	Con. (μg/mL)	Organism	ZOI (mm)	MIC (μg/mL)	MBC (μg/mL)	IC50 (μg/mL)	Mechanism	ref
α-Fe$_2$O$_3$	34	Quasi-spherical	FeCl$_3$, *P. guajava* leaf extracted, DW & acetone	GRS	Amp	25 μg (NPs) + 5 μg (antibiotic)	*Listeria monocytogenes* (ATCC 19115)	0	NR	NR	NR	Fe$_2$O$_3$ produced ROS, which broke the DNA strands, inactivated enzymes and led to lipid peroxidation. This activity triggered mechanisms such as penetration of cell membrane and induced oxidative stress which mediated cell death.	122
							Staphylococcus aureus (ATCC 49444)	24.42 ± 0.26					
							Salmonella typhimurium (ATCC 43174)	0					
							Candida albicans (KACC 30003)	10.33 ± 0.46					
							Candida albicans (KACC 30062)	16.15 ± 0.23					
							Candida glabrata (KBNO6P00368)	9.81 ± 0.57					
							Candida glochares (KACC 30061)	16.44 ± 0.21					
							Candida saitoana (KACC 41238)	10.01 ± 0.16					
					NR	20	*Escherichia coli*	29					
							Staphylococcus aureus	39					
						50	*Escherichia coli*	10					
							Staphylococcus aureus	13					
						100	*Escherichia coli*	12					
							Staphylococcus aureus	15					
Fe$_3$O$_4$	37.86	Spherical	FeCl$_3$, FeCl$_2$, *Zea mays L.*, & ear leaf extract.	GRS		Fe$_3$O$_4$ (25 μ) + kan (5 μ)	*Bacillus cereus* ATCC 13061	9.8 ± 0.34	NR	NR	NR	The ROS mediated by Fe$_3$O$_4$ NPs damaged DNA, protein and cellular membranes. Thus, resulted in bacterial cell death	146
							Escherichia coli ATCC 43890	18.86 ± 0.82					
							Listeria monocytogenes ATCC 19115	13.54 ± 0.30					
							Staphylococcus aureus ATCC 49444	13.09 ± 0.15					
							Salmonella typhimurium ATCC 43174	13.3 ± 0.47					
						Fe$_3$O$_4$ (25 μ) + Rif (5 μ)	*Bacillus cereus* ATCC 13061	0					

Table 2. continued

NPs	Particle size (nm)	Shape	Precursor	Synthesis method	Coating Material	Con. (μg/mL)	Organism	ZOI (mm)	MIC (μg/mL)	MBC (μg/mL)	IC50 (μg/mL)	Mechanism	ref
α-Fe$_2$O$_3$	20	Spherical	Fe(NO$_3$)$_3$·9H$_2$O, DW, & S. cordifolia extract.	GRS	NR	50	Escherichia coli ATCC 43890	0	NR	NR	NR	The ROS-mediated free radicals could disrupt the cell membrane via different interactions such as electrostatic, dipole, hydrogen, etc.	121
							Listeria monocytogenes ATCC 19115	0					
							Staphylococcus aureus ATCC 49444	20.90 ± 0.50					
							Salmonella typhimurium ATCC 43174	±0.34					
							Escherichia coli	11.33 ± 0.58					
							Bacillus subtilis	16 ± 1					
							Staphylococcus aureus	13.67 ± 0.58					
							Klebsiella pneumoniae	12 ± 1					

[a]NPs: Nanoparticles; Con.: Concentration; ZOI: zone of inhibition; ref: References; ROS: Reactive oxygen species; NR: Not reported; MIC: Minimum inhibitory concentration; MBC: Minimum bactericidal concentration; IC$_{50}$: Half maximal inhibitory concentration; FeCl$_3$,6H$_2$O: Ferric chloride hexahydrate; Fe (NO$_3$)$_3$·9H$_2$O: Ferric nitrate nonahydrate; DW: Deionized water; PEG: Poly(ethylene glycol); Kan: Kanamycin; Rif: Rifampicin; GRS: Green synthesis; GMAM: gray mangrove Avicennia marina; Amp: amphotericin; LPE: linear polyester; MH: Maize silky hairs; CCP: Leaves of Chinese cabbage; PMC: Psidium guajava-moringa composite; L-tyr: L-tyrosine; S. cordifolia: Sida cordifolia.

a gel. The polycondensation reaction generates a polymeric network that IONPs can retain. In most cases, nitrate precursors are utilized in SG methods for several key benefits, including uniformity in size and high levels of purity and quantity for IONPs.[119] For these reasons, IONPs produced through the SG method exhibit noteworthy antibacterial activity against various bacteria at varying concentrations. The SG method is widely utilized to synthesize doped metal IONPs; however, some research indicates the synthesis of IONPs through the SG method and observes their antibacterial activity against some Gram-negative and positive bacteria. For instance, Fe_3O_4 was generated through the SG procedure, and its antibacterial activity was observed at different concentrations ranging from 5 to 20 μg/mL on different Gram-negative and positive bacteria. IONPs at different concentrations exhibited 19 to 36 mm ZOI for *E. coli* and *B. cereus*[101] (Table 2). Additionally, Brahmbhatt et al.[102] conducted an antibiogram with Fe_3O_4 produced by SG and gave a visual aid for ZOI; however, the experiment lacked statistical analysis regarding the antibacterial activity of IONPs.

5.1.3. Other Chemical Synthesis Methods. IONPs can be synthesized using other chemically induced methods, including chemical precipitation, modified coprecipitation,[120] wet chemical, matrix-mediated method, hydrothermal, and laser ablation methods which are commercially available from several companies. In the modified coprecipitation method, cationic and anionic solutions are mixed for nucleation, and the aggregation of NPs is controlled by the pH and temperature.[120]

The HDT produces IONPs with excellent crystalline structure at high temperature and pressure in an aqueous solution. The method also enhanced magnetism, uniform size distribution, and reduced aggregation. As a result, the IONPs produced through thermal decomposition would exhibit exceptional stability, while their compact size would significantly boost their antimicrobial effectiveness. For example, when Fe_3O_4 NPs are synthesized using HDT, they show more substantial antibacterial effects on Gram-positive than Gram-negative bacteria. IONPs displayed a ZOI range of 12−28 mm for Gram-positive and 12−22 mm for Gram-negative bacteria.[68] Therefore, IONPs synthesized through the HDT method demonstrated satisfactory antibacterial activity.

The liquid solution is subjected to pulsed laser beams to conduct the laser ablation synthesis procedure for synthesizing IONPs.[121] The method consists of a high-power laser submerged in an aqueous solution, targeting the precursors. In this method, IONPs can be obtained using a single-step procedure. The IONPs produced using these methods are entirely surfactant-free, resulting in exceptional stability and purity. Thus, IONPs produced through the PLS method displayed moderate antibacterial activity against Gram-positive and Gram-negative bacteria.[103]

5.1.4. GRS Method. GRS refers to a method where the biology-mediated synthesis of NPs is conducted. A range of biological elements, including microorganisms and leaf extracts like Chinese cabbage, mare silk, *Psidium guajava*,[122] *Punica granatum, Zea mays*,[123] and *Sida cordifolia*[91] could complete the synthesis procedure. This synthesis procedure is slightly modified,[121] where the extraction of biological components is used as a reducing or stabilizing agent that is considered less toxic, convenient, economical, simple, eco-friendly, and biocompatible.[30,71,99,124,125] IONPs synthesized through GRS acquire significant antibacterial activity against pathogenic

bacteria compared to other chemical-induced synthesis methods[123,125] due to the inherent therapeutic characteristics of the plant extracts (Table 2).[85,126−128]

According to a study by Singh et al.[85] the antimicrobial effectiveness of the MNPs depends on two parameters: (i) the precursors used to synthesize the nanomaterials and (ii) the size of the particles. The plant extracts utilized in synthesizing IONPs for antibacterial purposes consist of phytochemicals that possess preexisting therapeutic or medicinal capabilities. As a result, IONPs produced by GRS using the green precursors induce a combined antimicrobial action, which exhibits a comparatively heightened antibacterial activity than other chemically induced methods.[129,130] *Purpureocillium lilacinum* was used to synthesize Fe_2O_3 and showed antibacterial activity against Gram-positive and negative bacteria, especially Gram-positive bacteria.[131] This fungus is a well-known biocontrol agent used to produce leucinostatin antibiotics, which could be used against bacteria and fungus.[132] Again, *penicillium spp.*,[133] *Citrus* leaf extract,[134] *Tamarix aphylla* extract,[135] *Thymbra spicata* leaf extract,[136] *Lawsone inermis* extract,[137] and *P. guajava* leaf extract[138] possess prior antimicrobial activity. Hammad et al.[131] reported that Fe_2O_3 NPs generated by *Capparis zeylanica* leaf extract showed approximately 23 and 22 mm ZOI for *S. aureus* and *P. aeruginosa*, respectively. Again, IONPs were synthesized using *Penicillium spp* and displayed an approximate ZOI of 12 and 11 mm for similar organisms.[139] In both cases, the IONPs generated by *Capparis zeylanica* showed a more pronounced antibacterial effect.

IONPs synthesized using *Citrus* leaf extracts inhibit the growth of *B. cereus, K. pneumoniae*, and *B. subtilis.* Similarly, Fe_2O_3 NPs produced from *Tamarix aphylla* and *Thymbra spicata* extracts are able to eradicate *E. coli* and *S. aureus* bacteria in a dose-dependent manner. Additionally, modifying the surface of IONPs with different types of antimicrobial agents, including kanamycin (Kan), rifampicin (Rif), and amphotericin (Amp), has proven to be more effective against microbes than the bare particles synthesized by GRS.[69,141,142] Moreover, IONPs synthesized via the GRS method have demonstrated notable antibacterial efficacy in compared to chemically synthesized methods (Tables 1, 2).

5.2. Size. IONPs have distinctive antimicrobial properties due to their physical and chemical characteristics, including the large surface area-to-volume ratio, superparamagnetic properties, and self-assembly.[147,148] These attributes are relevant to various factors, including their size, which influences their antimicrobial properties. Different synthesis procedures can influence the range of effective sizes of the IONPs.[149] Moreover, small IONPs exhibited enhanced stability and a higher surface-area-to-volume ratio, increasing free energy content, surface charge, and reactivity. The surface reacts with the microbes to achieve content stabilization, effectively diffusing into the cytoplasmic region and permeating the bacterial cell wall or membrane.[9,95,150] The heightened reactivity exhibited by NPs of smaller dimensions leads to an augmented generation of ROS, thereby promoting electron transfer due to the quantum confinement effect.[151] Furthermore, to optimally utilize drug delivery and antibacterial activity, the NPs' size should be less than 100 nm, commonly referred to as superparamagnetic iron oxide nanoparticles (SPIONs).[152−157]

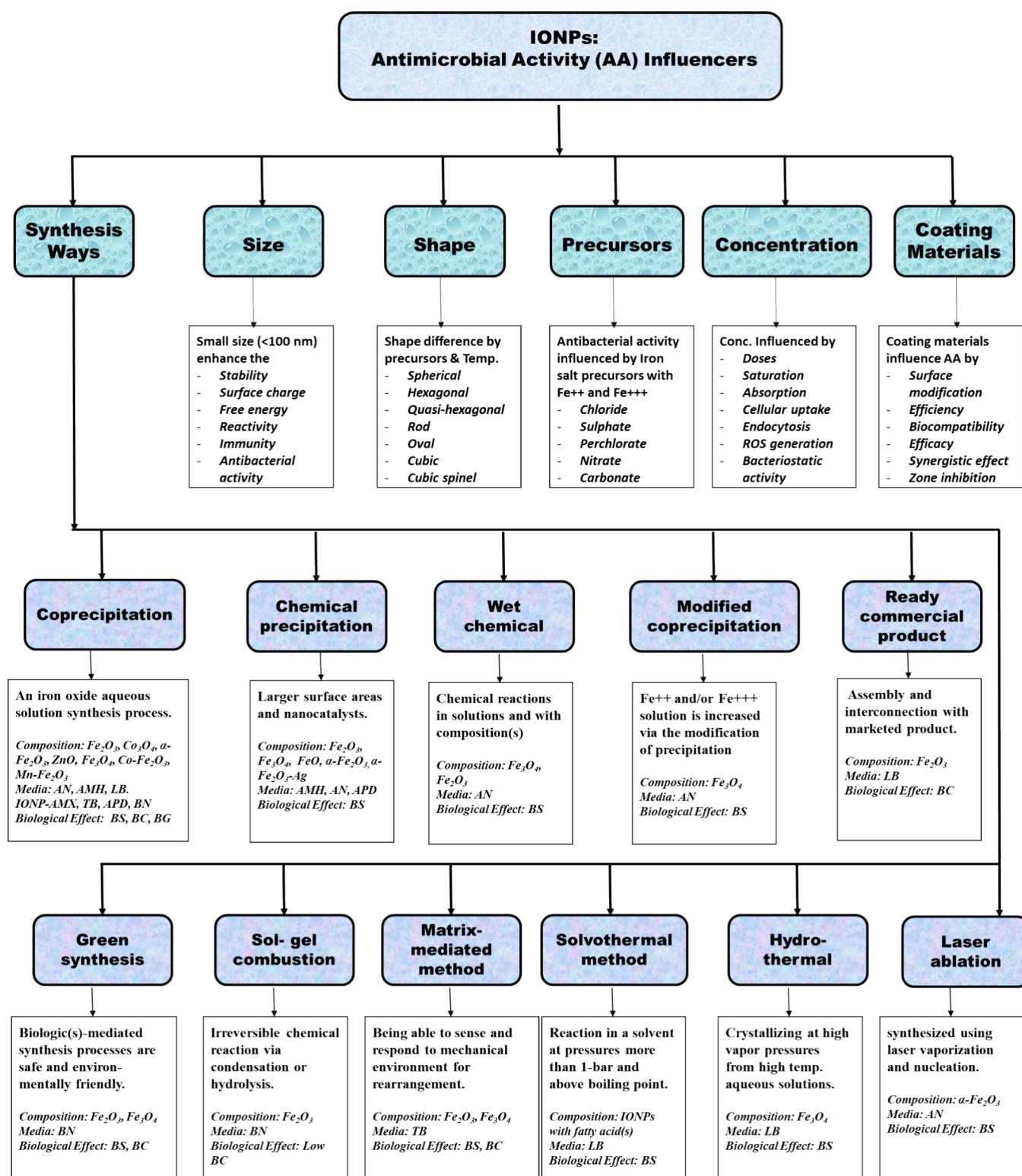Generally, smaller IONPs show enhanced antimicrobial activity compared to larger IONPs. IONPs with a size of

**IONPs:
Antimicrobial Activity (AA) Influencers**

Synthesis Ways	Size	Shape	Precursors	Concentration	Coating Materials

Size

Small size (<100 nm) enhance the
- *Stability*
- *Surface charge*
- *Free energy*
- *Reactivity*
- *Immunity*
- *Antibacterial activity*

Shape

Shape difference by precursors & Temp.
- *Spherical*
- *Hexagonal*
- *Quasi-hexagonal*
- *Rod*
- *Oval*
- *Cubic*
- *Cubic spinel*

Precursors

Antibacterial activity influenced by Iron salt precursors with Fe++ and Fe+++
- *Chloride*
- *Sulphate*
- *Perchlorate*
- *Nitrate*
- *Carbonate*

Concentration

Conc. Influenced by
- *Doses*
- *Saturation*
- *Absorption*
- *Cellular uptake*
- *Endocytosis*
- *ROS generation*
- *Bacteriostatic activity*

Coating Materials

Coating materials influence AA by
- *Surface modification*
- *Efficiency*
- *Biocompatibility*
- *Efficacy*
- *Synergistic effect*
- *Zone inhibition*

Coprecipitation

An iron oxide aqueous solution synthesis process.

Composition: Fe_2O_3, Co_3O_4, α-Fe_2O_3, ZnO, Fe_3O_4, Co-Fe_2O_3, Mn-Fe_2O_3
Media: AN, AMH, LB. IONP-AMX, TB, APD, BN
Biological Effect: BS, BC, BG

Chemical precipitation

Larger surface areas and nanocatalysts.

Composition: Fe_2O_3, Fe_3O_4, FeO, α-Fe_2O_3, α-Fe_2O_3-Ag
Media: AMH, AN, APD
Biological Effect: BS

Wet chemical

Chemical reactions in solutions and with composition(s)

Composition: Fe_3O_4, Fe_2O_3
Media: AN
Biological Effect: BS

Modified coprecipitation

Fe++ and/or Fe+++ solution is increased via the modification of precipitation

Composition: Fe_3O_4
Media: AN
Biological Effect: BS

Ready commercial product

Assembly and interconnection with marketed product.

Composition: Fe_2O_3
Media: LB
Biological Effect: BC

Green synthesis

Biologic(s)-mediated synthesis processes are safe and environmentally friendly.

Composition: Fe_2O_3, Fe_3O_4
Media: BN
Biological Effect: BS, BC

Sol-gel combustion

Irreversible chemical reaction via condensation or hydrolysis.

Composition: Fe_2O_3
Media: BN
Biological Effect: Low BC

Matrix-mediated method

Being able to sense and respond to mechanical environment for rearrangement.

Composition: Fe_2O_3, Fe_3O_4
Media: TB
Biological Effect: BS, BC

Solvothermal method

Reaction in a solvent at pressures more than 1-bar and above boiling point.

Composition: IONPs with fatty acid(s)
Media: LB
Biological Effect: BS

Hydro-thermal

Crystallizing at high vapor pressures from high temp. aqueous solutions.

Composition: Fe_3O_4
Media: LB
Biological Effect: BS

Laser ablation

synthesized using laser vaporization and nucleation.

Composition: α-Fe_2O_3
Media: AN
Biological Effect: BS

Figure 2. An illustration of the numerous IONPs parameters that influenced the antibacterial activity. Here, AA: antimicrobial activity, AN: agar nutrient, AMH: agar Mueller-Hinton solution, LB: lysogenic broth, Amx: amoxicillin, TB: tryptic-soy broth, APD: agar potato dextrose solution, BN: broth of nutrient, BS: bacteriostatic effect, BC: bactericidal effect, and BG: bacterial growth.

around 10−100 nm display moderate antibacterial activity against a range of bacteria. For instance, hematite with a size ranging from 13.13 to 24.93 nm showed excellent antibacterial activity, where the recorded ZOI for *E. coli* was 23 mm.[131] Again, hematite with a slightly large size like 28.17 nm showed decreased bacteriostatic activity with a 19.5 mm ZOI.[140] The

size difference between the two hematites was approximately 3−5 nm, influencing the antibacterial efficacy. Moreover, magnetite also showed significant antibacterial activity against numerous bacteria in sizes ranging from 8 to 260 nm. Moreover, where the size of IONPs is less than 10 nm and higher than 100 nm, the antibacterial activity of the IONPs

decreases, such as IONPs ranging from 3.31 to 10 nm shows a ZOI of 11 ± 0.6 mm and 40 nm sized IONPs showed 21.5 ± 0.36 mm for *K. pneumoniae*.[69,139] Nevertheless, the antibacterial efficacy of this diverse range of IONPs lack to consistently correlate with their size due to other intrinsic parameters like precursors, synthesis methods, and coating materials (Figure 2). For instance, the effectiveness of antibacterial agents can vary depending on their dimensions and other inherent factors, like the materials used for their coating. In the case of both coated and uncoated IONPs, it was observed that their sizes varied within a range of approximately 6−254 nm and 3−200 nm, respectively, when employing the COP and GRS methods. However, it is often observed that smaller-sized IONPs tend to interact more frequently with pathogenic bacteria, resulting in dose reduction.[158−161] Consequently, smaller IONPs exhibit a greater level of antibacterial activity.[162−164]

5.3. Shape. The shape of the IONPs is crucial for their antibacterial activity. Numerous papers have documented different shapes of IONPs, such as hexagonal, quasi-hexagonal, and spherical. Interestingly, the majority of the research papers focused on the prevalence of spherical-shaped IONPs. These morphological differences are achieved by modifying the precursor molecules and temperature.[165] Diverse-shaped IONPs utilize different approaches to interact with bacteria; hexagonal IONPs are larger compared to spherical ones. As a result, the hexagonal IONPs interact with the bacterial cell wall due to their sharp edges, which results in cell wall distortion.[166,167] However, the spherical-shaped IONPs could diffuse into the intercellular space. Additionally, there is empirical evidence that displays this particular variant is not effective against all types of bacteria.[168−170] A study revealed that nanoparticles with a spherical shape exhibit the highest level of effectiveness in combating bacterial infections.[171] Moreover, it is evident that spherical IONPs exhibit the most potent antibacterial activity. For example, when studying hexagonal IONPs using the COP method, the findings showed an average ZOI between 11 and 12 mm (Tables 1 & 2).[59] Conversely, IONPs with a spherical shape showed a 17 mm inhibition.[93] A larger ZOI suggests that spherical IONPs have superior antibacterial activity than their hexagonal counterparts.

5.4. Concentration. The concentration of IONPs significantly affects their antimicrobial action, depending on various aspects such as dose, saturation effect, and cellular absorption. The antimicrobial activity of IONPs frequently depends on their dose.[172,173] With the increased concentration, the bacterial cell surface may become saturated with IONPs, thereby increasing the probability of cellular uptake and consequently enhancing antimicrobial effects.[174,175] Nevertheless, saturation may impose a constraint on IONPs, thereby diminishing their antibacterial effectiveness.[176−179]

The antimicrobial efficacy of the IONPs against pathogenic microorganisms is contingent upon their concentration. Due to the increase in concentration, a corresponding escalation in bacteriostatic activity was observed. Numerous studies have displayed the dose-dependent effect of IONPs against pathogenic microorganisms. For instance, Mehrabi et al.[68] have examined the dose-dependent effect of IONPs on several pathogenic bacteria, where the antimicrobial activity of IONPs was observed at different concentrations, at the lowest concentration of 25 μg/mL, approximately 20 mm and 15 mm, and at the highest concentration of 200 μg/mL, 28 mm

and 22 mm ZOI for *S. aureus* and *K. pneumonia*. The elevated concentration would indicate a higher possibility of endocytosis and enhanced generation of ROS. The increased production of ROS would improve oxidative stress and quickly eliminate microbial cells. Another study displayed a concentration-dependent approach of Fe_2O_3 NPs against the bacteria *B. subtilis, S. aureus, E. coli,* and *S. typhi* (Table 1). At a 400 μg/mL concentration, the observed zone diameters were 11, 12, and 19 mm. However, at a higher concentration of 800 μg/mL, the observed zone diameters were 15, 16, 17, and 21 mm, respectively.[122] The remarked zone diameter values exhibited a proportional relationship with the varying concentrations, whereby lower concentrations corresponded to smaller ZOI. In comparison, higher concentrations were associated with augmented zones of inhibition. Sharaf et al.[87] stated that the concentration of RHL-coated IONPs determines whether various bacterial strains exhibit bactericidal or bacteriostatic activity. The MIC and MBC concentrations of IONPs exhibited variation against distinct isolates of *S. aureus*, including MRSA, VRSA, and MSSA, which were 16, 32, and 64 μg/mL, respectively. Different isolates of *E. coli* bacteria also displayed multiple concentrations of MIC and MBC; hence, the increased concentration would elevate the antibacterial activity of the IONPs.

5.5. Precursors. IONPs can be synthesized using different iron salt precursors, e.g., chloride, sulfate, perchlorates, and nitrate salt precursors.[180] Moreover, the antimicrobial activity of IONPs can be significantly influenced by the utilization of distinct iron salt precursors during their synthesis. It is worth noting that the resulting IONPs exhibit varying levels of antimicrobial activity depending on the specific salts used during synthesis. The Fe_3O_4 sample, synthesized through the utilization of $FeCl_3·6H_2O$ and $FeCl_2·4H_2O$, demonstrated a notable ZOI of 20 mm[68] while IONPs synthesized by $Fe(NO_3)_3·9H_2O$ showed a 9 mm ZOI[99] for *S. aureus*. Furthermore, the iron precursor employed in the green synthesis process may also impact the bacteriostatic activity of the synthesized compounds. Fe_2O_3 NPs were synthesized utilizing various iron precursors via a sustainable and environmentally friendly approach known as green synthesis. Hematite was synthesized individually, employing $FeCl_3·6H_2O$ and $FeSO_4$ as precursors, respectively. IONPs that were synthesized using $FeCl_3·6H_2O$ exhibited a zone diameter of 21 and 23 mm[140] while IONPs synthesized by $FeSO_4$ exhibited a ZOI of 26, 19.5, and 17 mm for *S. aureus, E. coli*, and *P. aeruginosa,* respectively.[131] The provided data (Table 1) indicated that IONPs produced using chloride salts exhibited greater efficacy compared to those synthesized using sulfate salt when tested against *E. coli* and *P. aeruginosa*. However, the IONPs synthesized using sulfate salt demonstrated superior effectiveness against *S. aureus*. Additionally, IONPs synthesized utilizing a chloride precursor exhibited a zone diameter measuring 26 and 21.5 mm, respectively.[69] On the contrary, $Fe(NO_3)_3$ precursor-derived IONPs showed 12 and 16 mm, ZOI for *K. pneumoniae* and *B. subtilis,* respectively.[121] In this case, the chloride precursor was highly influential in inhibiting the microorganisms compared to the IONPs produced by nitrate salt. Hence, the inspection suggested that different precursors used to synthesize IONPs would influence their antimicrobial properties.[181−183]

5.6. Surface Modification to Enhance Antibacterial Activity of IONPs. The surface modification of IONPs could influence their physical, chemical, and biological character-

istics. There are various methods to modify the surface of IONPs; however, using coating techniques to modify the surface of IONPs is highly effective. Moreover, the application areas would vary according to the coating materials utilized on IONPs because the properties of the coating materials alter the activity of the IONPs. Several studies have been conducted which offer valuable insights into surface modification that increases the antibacterial activity of IONPs.[184−187] Hence, IONPs coated with antimicrobial agents such as gentamicin,[98] Kan, Rif, Amp,[188] poly(vinyl alcohol), teicoplanin,[94] dimethylformamide, sodium dodecyl sulfate,[189] and gallic acid (GA) form a nanocomplex, then these complexes tend to exhibit a combined effect against pathogenic bacteria (Tables 1 & 2). For instance, the bare IONPs exhibited ZOI, and the diameters were 17.33 ± 0.57 mm, 17.51 ± 0.57 mm, and 17.66 ± 0.57 mm while the IONPs conjugated with PEG+GEN demonstrated enhanced antimicrobial activity, with zone diameters of 23.66 ± 0.57 mm, 25.66 ± 0.57 mm, and 26.33 ± 0.57 mm against *S. epidermidis*, *P. mirabilis*, and *A. baumannii*, respectively. Hence, an increase in the diameter of the inhibitory zone by 7 mm was observed, which is attributed to the bacteriostatic properties exhibited by the coating material.[93] Additionally, similar results were observed as antibiotics, beta-cyclodextrin,[100] and L-tyrosine were coated on IONPs.[143]

The coating material used to improve the antibacterial activity must have inherent bacteriostatic qualities; hence, utilizing various coating materials would influence the antibacterial activity of IONPs. For instance, Kan-coated IONPs showed an inhibition zone diameter of 10.35 ± 0.17 mm, 18.44 ± 0.41 mm, 16 ± 0.86 mm, and 13.17 ± 0.26 mm while Rif-coated IONPs exhibited 9.36 ± 0.28 mm, 9.62 ± 0.28 mm, and 21.99 ± 1.32 mm against *B. cereus*, *E. coli*, *L. monocytogenes*, *S. aureus*, and *S. typhimurium*, respectively.[123] Therefore, the different coating materials exhibited different ZOI. Additionally, utilizing multiple coating materials would display an increase in ZOI. For instance, the MICs of RHL-coated IONPs against various strains were found to be 4 μg/mL, 16 μg/mL, 32 μg/mL, 32 μg/mL, 64 μg/mL, and 64 μg/mL, while the MICs of RHL, PVA, GA, and p-CoA-coated IONPs against the same strains were determined to be 1 μg/mL, 4 μg/mL, 16 μg/mL, 16 μg/mL, 32 μg/mL, and 32 μg/mL *E. coli* (O26:H11), MSSA, *E. coli* (O78:H10), MRSA, *E. coli* (O157:H7), and VRSA, respectively. Hence, coating IONPs with multiple materials reduced the MIC dose to almost half against pathogenic bacteria compared to the MIC of single-coated IONPs. The coating materials RHL, PVA, GA, and p-CoA have significant antimicrobial properties as well as specific mechanisms to inhibit microbial cells.[87] As a result, after coating them with IONPs, the individual materials started exhibiting their bacteriostatic mechanisms and the antimicrobial activity of the whole nanocomplex increased. As these coated IONPs complexes have displayed enhanced antimicrobial activity compared to bare IONPs, it is conclusive to state that the surface modifications of the IONPs would enhance their antimicrobial activity.[190,191]

Another approach could be doping impurities. It refers to the intentional introduction of specific foreign material into the lattice structure of the mother sample. Doping at various ratios to the other sample Fe_3O_4 could increase the antimicrobial activity. Since the dopant atom would influence the physicochemical properties of the IONPs, it would increase the interaction with the microorganism.[192] Additionally,

IONPs can achieve magnetic characteristics from dopant atoms, which could create severe vibration and damage the elasticity of the cell membrane and rupture the cells.[189,191,192] Therefore, doping would increase the antibacterial activity of IONPs.

6. ANTIMICROBIAL MECHANISMS OF IONPs

Studies have shown that IONPs have a moderate antimicrobial effect on various bacteria that are susceptible to it. In-depth research is being carried out to gain insights into the antibacterial mechanisms of IONPs. Until this point, these mechanisms involved the generation of ROS through the Fenton reaction leading to lipid peroxidation, DNA damage, and protein damage. Additionally, the presence of free radicals causes lipid peroxidation, which in turn initiates ferroptosis, resulting in oxidative stress and, ultimately, cell death.[193,194] Additionally, IONPs exhibit electrostatic interaction with bacteria and hinder cellular integrity. Thus far, these mentioned mechanistic understandings of IONPs have been theorized.

6.1. Cell Membrane Disruption.
The cellular membrane of bacteria is composed of a bilayer of phospholipids interspersed with specialized proteins embedded within it. The semipermeable membrane exhibits hydrophilic polar heads and covalently linked hydrophobic nonpolar tails with ion channels.[49] Bacterial cell membranes are negatively charged due to highly electronegative groups on their constituent phospholipids and lipopolysaccharides.[195] IONPs can have either a positive or negative charge, leading to electrostatic interactions with the bacterial cell membrane. The antibacterial activity resulting from electrostatic interaction can differ depending on the surface charge of IONPs and the specific bacterial species. The surface charge of the IONPs interacts with the bacterial cell membrane through electrostatic attraction or repulsion and disrupts their integrity by increasing cell permeability, which allows frequent ion exchange into the cell and leads to cell death.[196] Additionally, IONPs adhere to the bacterial cell membrane, and due to their nanosized nature and high surface-to-volume ratio, they can cause physical disruption to the cell membrane.[30,149]

Generally, synthesized IONPs consist of an overall negative charge due to the inherited hydroxyl group. However, the surface charge of the IONPs is dependent on the pH, being positive at low pH and negative at high pH. In both states, IONPs exhibit antibacterial activity through electrostatic attraction and repulsion. Positively charged iron ions present in IONPs have the potential to exert an influence on the integrity of cell membranes. An interruption occurs via electrostatic forces, upon the interaction of the iron ion with the cell wall. The metal ion then either attaches itself to the bacterial cell's membranes or uses protein channels to enter the intracellular space.[197]

6.2. ROS Production.
One of the most auspicious antibacterial mechanisms exhibited by IONPs involves the generation of ROS through photocatalysis, cellular aerobic metabolism, and the Fenton reaction. ROS can be generated by reducing O_2 and the oxidation of H_2O.[198] In photocatalysis, UV light is required to generate ROS such as hydrogen peroxide (H_2O_2), hydroxy radical (^-OH), and superoxide ($\cdot O_2^-$).[199,200] However, ROS generated through the Fenton reaction do not require any solar light. The Fe^{3+} is reduced to Fe^{2+} by accepting an electron in the Fenton reaction. As Fe^{2+} is unstable in the presence of O_2, it is rapidly oxidized and
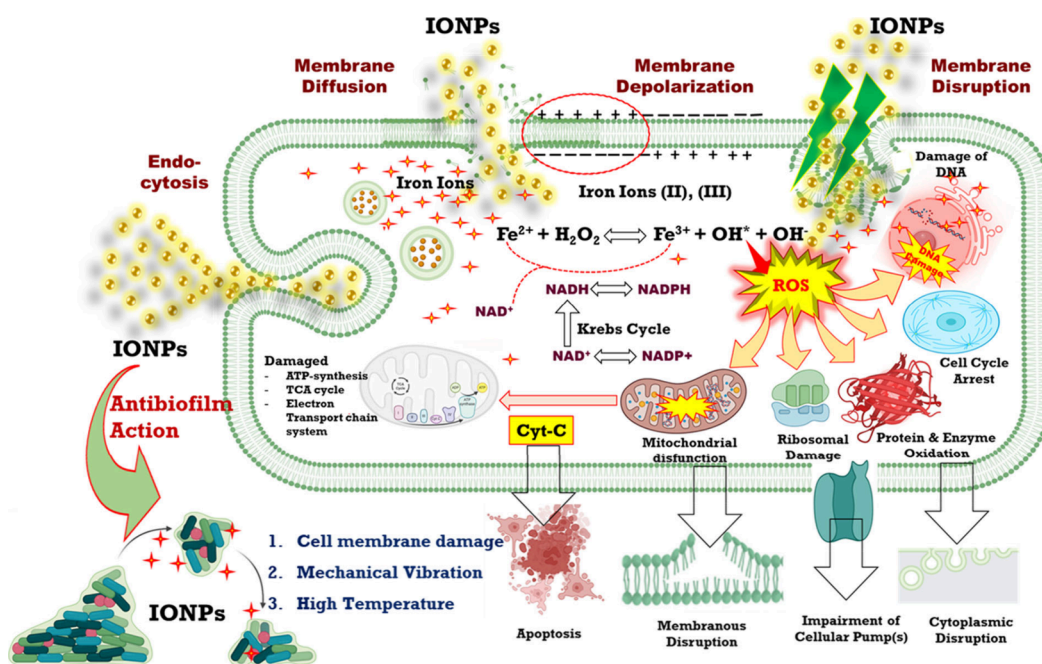
Figure 3. A diagrammatic illustration of IONPs antibacterial and antibiofilm mechanisms. IONPs trigger oxidative stress and cell lysis by generating ROS, altering membrane depolarization, damaging protein or nucleic acid, inactivating enzymes, damaging mitochondria or ribosome, impairing efflux pump, disrupting cytoplasm and cell membrane. ROS: Reactive oxygen species; IONPs: Iron oxide nanoparticles.

produces $\cdot O_2^-$, reduces the Fe^{3+} to Fe^{2+}, and their dismutation continuously produces H_2O_2. The reduced Fe^{2+} increases and reacts with H_2O_2, generating free radicals such as $-OH$.[201−204]

The following reaction displays a generalized Fenton reaction for generating ROS.

$$Fe^{3+} + e^- \rightarrow Fe^{2+}$$

$$Fe^{2+} + O_2 \rightarrow Fe^{3+} + \cdot O_2^-$$

$$Fe^{2+} + H_2O_2 \rightarrow Fe^{3+} + \cdot OH + OH^-$$
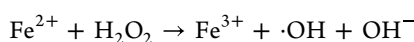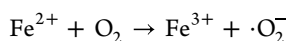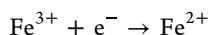
These ROS inhibited bacterial growth in various ways, including peroxidation of lipids in the cell membrane, damaging DNA, inhibiting replication, transcription, and translation.[196,205−211] Additionally, free radicals can reduce the antioxidant system, including enzymes and natural elements, *e.g.,* catalase, peroxidase, ascorbic acid, and carotenes, which could deactivate enzymes and inhibit bacterial growth. Hence, ROS were held responsible for a cascade of malfunctions that resulted in bacterial mortality by inducing oxidative stress in the cell (Figure 3).

6.3. Damage to Cellular Content. The cellular composition of a bacterial cell is primarily composed of DNA, proteins, and lipids. Once the IONPs have successfully traversed the cellular membrane, they possess the capability to engage with various constituents within the cytoplasmic milieu. Damage to DNA and proteins induced by reactive oxygen species (ROS) is commonly investigated in the field. However, it is worth noting that certain studies have suggested alternative outcomes based on the specific characteristics of ROS, such as their size, shape, and concentration.[212] Although IONP's toxicity is suggested, it also exhibits apparent genotoxic properties. The IONPs demonstrated that they directly intercalate with DNA, breaking DNA strands.[213,214] Additionally, the IONPs may interact with the proteins and enzymes necessary for ATP synthesis.[212] These ions might obstruct

ribosomal activities and stop them from synthesizing proteins. Gradually, interacting with the cytoplasmic content, replication, transcription, and translation might be inhibited by IONPs, which also have antibacterial properties.[23,196,215]

6.4. Enzyme Inactivation. IONPs could inhibit bacterial growth by interfering with the enzymatic activities of the microbial cells. IONPs hinder the enzymatic pathways and inhibit bacterial growth by binding with the enzyme, denaturing the enzyme, interfering with the cofactors, and disrupting energy production.[216,217] IONPs can interact with either the surface or the active site of enzymes. Due to their nonspecific binding mechanism exhibited by IONPs, they possess the potential to function as irreversible enzyme inhibitors. IONPs exhibit diminutive dimensions, rendering them at the nanoscale level. Additionally, a molecular entity exhibits the inherent capability to act as an enzymatic inhibitor because it can imitate the native substrate and form a binding interaction with the enzyme's catalytic site.[218]

6.5. Efflux Pump. IONPs could inhibit bacterial growth by interacting with efflux pumps. The efflux pump is a transport system localized in the cytoplasmic membrane to expel harmful substances from the cell. So, bacteriostatic activity could be achieved by preventing the release of the efflux pump. There are possible mechanisms by which an efflux pump could be inhibited. The first possible mechanism to inhibit the efflux pump is the direct binding of IONPs to the efflux pump. The disruption of efflux kinetics could be another mechanism that inhibits microbial cell growth.[219] To comprehensively grasp the impact of the efflux pump on drug resistance, it is imperative to ascertain the kinetic constants. Hence, perturbing the efflux kinetics would exert an impact on the MDR efflux pump.[219] The initial mechanism elucidated the noteworthy potential of direct binding between IONPs and an efflux pump to impede the proliferation of microbial cells. Nevertheless, the interaction between IONPs and the efflux pump may give rise to certain challenges. One of the prevailing concerns pertains

to the dimensions of the efflux pump and its inert response in the face of the IONPs.[220] Therefore, IONPs might interact with the other membrane proteins to become associated with a nearby efflux pump.[221]

7. TOXICITY OF IONPs

The utilization of IONPs as a therapeutic agent has become increasingly frequent in the clinical field. Therefore, conducting a cytotoxicity assay to assess the biocompatibility of IONPs both in vitro and in vivo is crucial. Frequently used techniques for investigating the toxicity and assessing the biocompatibility of IONPs in vitro include cell viability assay, LDH assay to examine cell membrane integrity, MTT assay to evaluate mitochondrial function, immunohistochemistry to detect markers of apoptosis, hemolysis assay, microscopic analysis of intracellular localization, and genotoxicity assessment for specific cell expression.[222−228] The toxicity of IONPs is influenced by various parameters, including their dimensions, morphology, surface coating, method of administration, attached peptide, medication, and targeting agents.[229−231] Smaller IONPs with a size lower than 10 nm are generally more hazardous than larger ones due to their higher surface area, which creates a higher possibility of penetrating the cells.[232] However, in the case of an in vivo system, smaller IONPs are rapidly eliminated through extravasation and renal clearance, whereas the spleen captures the larger ones through mechanical filtration.[233−235] Moreover, the surface charge can significantly influence the cytotoxicity of IONPs. The membrane potential of a cell is usually negative, and the surface charge of the IONPs is negative and sometimes positive; their interaction can be repulsive or attractive. The smaller NPs with a high surface area would have a higher change in ratio, increasing the electrostatic interaction between the cell and IONPs and damaging them. Furthermore, several coating materials are able to influence the toxicity of IONPs. For instance, longer exposure to IONPs could induce cytotoxicity due to the production of free radicals. However, toxic effects may be neutralized through PEGylation.[236] PEG forms a hydrophilic barrier around IONPs, reducing the interaction between IONPs and cell membranes. More importantly, PEG coating enhances their antimicrobial activity and biocompatibility. Additionally, IONPs are less likely to cause significant health problems since Fe^{3+} is widely found in the human body. Hence, the release of the iron would not cause any major side effects in the in vivo system.[237−239]

8. LIMITATIONS AND FUTURE DIRECTIONS

IONPs have moderate antibacterial activity due to several factors, including their interaction mechanisms, nutrient deprivation, varying susceptibility, dose determination, and cytotoxicity.[240−242] IONPs interact with microbes through different mechanisms; however, these mechanisms depend on their size. Smaller IONPs have a larger surface area and can interact physically and more frequently with the bacterial cell membrane.[243] On the contrary, the larger particles are not able to interact much frequently. Due to having a smaller surface area to volume ratio, their determined dose to eradicate bacteria increases.[244,245] Moreover, dose determination becomes extremely difficult when the pathogens have variable susceptibility. Furthermore, IONPs are able to interfere with microbial nutrient uptake, as most pathogenic bacteria require iron for their growth and survival.[246,247] Additionally, a few of

the IONPs interact with cells, producing ROS that can be toxic for cells and induce pro-inflammatory mediators.[248−251]

Though IONPs have several limitations as therapeutic agents, these limitations can be minimized using biocompatible precursors and surface modification. For instance, in the GRS synthesis method, bioreductants, which consist of phytochemicals with prior antimicrobial activity, are used instead of chemicals.[252,253] Therefore, a combined mechanism is initiated against eliminating bacteria; hence, the potency of IONPs increases.[254] Additionally, surface modification approaches can help address IONPs' main drawbacks, such as stability issues, cytotoxicity, biocompatibility, and moderate antibacterial activity.[149,255] Biopolymers such as PEG and chitosan are used as coating material to modify the surface of IONPs.[256,257] These biopolymers consist of antibacterial and biocompatible properties.[258] Hence, surface-modified IONPs would be more potent as an antimicrobial agent because these biopolymers would compress the size of the particles and increase the surface area to volume ratio, resulting in a combined mechanism against pathogenic bacteria and acquiring increased bioavailability while keeping the cytotoxicity to a minimum by reducing the interaction between IONPs and tissues.[259−261]

IONPs exhibit moderate antibacterial activity as a therapeutic agent against pathogenic bacteria since the dose of IONPs would vary depending on the bacterial species, size of IONPs, and ROS production capabilities. For better and more precise outcomes, the GRS synthesis method and surface modification can be utilized to produce stable IONPs with enhanced biocompatibility and antibacterial activity. Furthermore, IONPs can be used in different clinical sectors, including cancer detection and treatment, magnetic hyperthermia, multimodal imaging, soil and water purifications, and biosensors.[42,196,262,263]

9. CONCLUSION

The antibacterial activity of the bare and coated IONPs depends on the synthesis methods, size, concentration, precursors, surface charge, and the materials used for coating. Among several synthesis methods, IONPs synthesized through GRS exhibited notable antibacterial efficacy. The phytochemicals with prior antimicrobial properties used in producing IONPs displayed a combined mechanism against bacteria. Additionally, IONPs expressed moderate antibacterial activity within the size range of approximately 10−100 nm. They exhibited higher cellular uptake and efficient antibacterial activity within this range, while IONPs with sizes smaller than 10 nm were less effective against bacteria. Furthermore, their properties to inhibit bacteria depend on their diminutive dimensions, and spherical-shaped IONPs show more significant potential for inhibiting bacteria than other shapes. Moreover, depending on the utilization of different iron salt precursors (e.g., sulfate, chloride, and nitrate) the antibacterial properties of IONPs vary. Among all the iron salt precursors, chloride salt has been proven to be the most effective precursor utilized to synthesize IONPs as an antibacterial agent. Although IONPs are used as therapeutic agents, they show moderate antibacterial activity. The moderate activities are increased by using different biopolymers (e.g., PEG, chitosan, L-try, antibiotics) as coating material. Surface modification via biocompatible coating material or drug candidates would increase stability, enhance biocompatibility, and simultaneously augment their antibacterial efficacy to address the pressing issue of infectious diseases caused by AMR organisms.

■ AUTHOR INFORMATION

Corresponding Authors

Md Mahamudul Hasan Rumon − *Department of Mathematics and Natural Sciences, Brac University, Dhaka 1212, Bangladesh;* orcid.org/0000-0002-0459-5035; Email: mhrumon.ku@gmail.com

Md Salman Shakil − *Department of Mathematics and Natural Sciences, Brac University, Dhaka 1212, Bangladesh;* orcid.org/0000-0002-8922-9500; Email: salman.shakil@bracu.ac.bd

Authors

Kishan Nandi Shoudho − *Department of Mathematics and Natural Sciences, Brac University, Dhaka 1212, Bangladesh; Department of Chemical Engineering, Bangladesh University of Engineering and Technology, Dhaka 1000, Bangladesh;* orcid.org/0009-0000-3962-7255

Shihab Uddin − *Department of Bioengineering, King Fahd University of Petroleum & Minerals, Dhahran 31261, Kingdom of Saudi Arabia;* orcid.org/0000-0001-5464-570X

Complete contact information is available at:
https://pubs.acs.org/10.1021/acsomega.4c02822

Author Contributions

Conceptualization, M.S.S.; writing original draft preparation, K.N.S., S.U., M.S.S., figure drawing S.U., M.H.R.; review and editing, S.U, M.H.R., and M.S.S.; project administration, M.S.S., M.H.R., and S.U.

Notes

The authors declare no competing financial interest.

■ REFERENCES

(1) Abushaheen, M. A.; Fatani, A. J.; Alosaimi, M.; Mansy, W.; George, M.; Acharya, S.; Rathod, S.; Divakar, D. D.; Jhugroo, C.; Vellappally, S.; et al. Antimicrobial resistance, mechanisms and its clinical significance. *Disease-a-Month* **2020**, *66* (6), No. 100971.

(2) Llor, C.; Bjerrum, L. Antimicrobial resistance: risk associated with antibiotic overuse and initiatives to reduce the problem. *Therapeutic advances in drug safety* **2014**, *5* (6), 229−241.

(3) Salam, M. A.; Al-Amin, M. Y.; Salam, M. T.; Pawar, J. S.; Akhter, N.; Rabaan, A. A.; Alqumber, M. A. In *Antimicrobial resistance: a growing serious threat for global public health*; Healthcare, MDPI, 2023; p 1946.

(4) Tang, K. W. K.; Millar, B. C.; Moore, J. E. Antimicrobial resistance (AMR). *British Journal of Biomedical Science* **2023**, *80*, No. 11387.

(5) Srakocic, S.; Biggers, A. How Do Bacteria Become Resistant to Antibiotics? In *Healthline*, 2022. https://www.healthline.com/health/antibiotics/how-do-bacteria-become-resistant-to-antibiotics#resistance

(6) Struelens, M. J. The epidemiology of antimicrobial resistance in hospital acquired infections: problems and possible solutions. *BMJ: British Medical Journal* **1998**, *317* (7159), 652−652.

(7) Materón, E. M.; Miyazaki, C. M.; Carr, O.; Joshi, N.; Picciani, P. H.; Dalmaschio, C. J.; Davis, F.; Shimizu, F. M. Magnetic nanoparticles in biomedical applications: A review. *Applied Surface Science Advances* **2021**, *6*, No. 100163.

(8) Shekoufeh, B.; Lotfipour, F.; Azhar, L. Magnetic nanoparticles for antimicrobial drug delivery. *Die Pharmazie-An International Journal of Pharmaceutical Sciences* **2012**, *67* (10), 817−821.

(9) Allafchian, A.; Hosseini, S. S. Antibacterial magnetic nanoparticles for therapeutics: a review. *IET nanobiotechnology* **2019**, *13* (8), 786−799.

(10) Cursaru, L. M.; Piticescu, R. M.; Dragut, D. V.; Tudor, I. A.; Kuncser, V.; Iacob, N.; Stoiciu, F. The Influence of Synthesis Parameters on Structural and Magnetic Properties of Iron Oxide Nanomaterials. *Nanomaterials* **2020**, *10* (1), 85.

(11) Ummah, A. M.; Peng, Y.-H.; Ho, C.-H. Structure, property and magneto-optical interaction of wide-band-gap layered magnetism near the Néel temperature with antiferromagnetic to paramagnetic transition. *FlatChem.* **2023**, *41*, No. 100536.

(12) Thakare, N. R.; Singh, R.; Talukdar, H.; Yadav, D.; Hazarika, S.; Ingole, P. G.; Ahn, Y.-H., Functionalization of biogenic and biomimetic magnetic nanosystems for biomedical applications. In *Functionalized Magnetic Nanosystems for Diagnostic Tools and Devices*; Elsevier, 2024; pp 229−255.

(13) Gupta, I.; Sirohi, S.; Roy, K. Strategies for functionalization of magnetic nanoparticles for biomedical applications. *Materials Today: Proceedings* **2023**, *72*, 2757−2767.

(14) Ahmadpour, F.; Ganjali, F.; Radinekiyan, F.; Eivazzadeh-Keihan, R.; Salimibani, M.; Bahreinizad, H.; Mahdavi, M.; Maleki, A. Fabrication and characterization of a novel magnetic nanostructure based on pectin−cellulose hydrogel for in vitro hyperthermia during cancer therapy. *RSC Adv.* **2024**, *14* (19), 13676−13684.

(15) Salam, M.; Zheng, H.; Liu, Y.; Zaib, A.; Rehman, S. A. U.; Riaz, N.; Eliw, M.; Hayat, F.; Li, H.; Wang, F. Effects of micro (nano) plastics on soil nutrient cycling: state of the knowledge. *Journal of Environmental Management* **2023**, *344*, No. 118437.

(16) Gupta, N.; Parsai, T.; Kulkarni, H. V. A review on the fate of micro and nano plastics (MNPs) and their implication in regulating nutrient cycling in constructed wetland systems. *Journal of Environmental Management* **2024**, *350*, No. 119559.

(17) Negrescu, A. M.; Killian, M. S.; Raghu, S. N. V.; Schmuki, P.; Mazare, A.; Cimpean, A. Metal Oxide Nanoparticles: Review of Synthesis, Characterization and Biological Effects. *J. Funct. Biomater.* **2022**, *13* (4), No. 274, DOI: 10.3390/jfb13040274.

(18) Fernandez, L.; Cima-Cabal, M. D.; Duarte, A. C.; Rodriguez, A.; Garcia, P.; Garcia-Suarez, M. D. M. Developing Diagnostic and Therapeutic Approaches to Bacterial Infections for a New Era: Implications of Globalization. *Antibiotics (Basel)* **2020**, *9* (12), 916.

(19) Dadfar, S. M.; Roemhild, K.; Drude, N. I.; von Stillfried, S.; Knüchel, R.; Kiessling, F.; Lammers, T. Iron oxide nanoparticles: Diagnostic, therapeutic and theranostic applications. *Adv. Drug Delivery Rev.* **2019**, *138*, 302−325.

(20) Łojewska, E.; Sakowicz, T. An Alternative to Antibiotics: Selected Methods to Combat Zoonotic Foodborne Bacterial Infections. *Curr. Microbiol.* **2021**, *78* (12), 4037−4037.

(21) Sánchez-López, E.; Gomes, D.; Esteruelas, G.; Bonilla, L.; Lopez-Machado, A. L.; Galindo, R.; Cano, A.; Espina, M.; Ettcheto, M.; Camins, A.; Silva, A. M.; Durazzo, A.; Santini, A.; Garcia, M. L.; Souto, E. B. Metal-Based Nanoparticles as Antimicrobial Agents: An Overview. *Nanomaterials* **2020**, *10* (2), 292−292.

(22) Shakil, M. S.; Bhuiya, M. S.; Morshed, M. R.; Babu, G.; Niloy, M. S.; Hossen, M. S.; Islam, M. A. Cobalt Ferrite Nanoparticle's Safety in Biomedical and Agricultural Applications: A Review of Recent Progress. *Curr. Med. Chem.* **2023**, *30* (15), 1756−1775.

(23) Karnwal, A.; Kumar, G.; Pant, G.; Hossain, K.; Ahmad, A.; Alshammari, M. B. Perspectives on Usage of Functional Nanomaterials in Antimicrobial Therapy for Antibiotic-Resistant Bacterial Infections. *ACS Omega* **2023**, *8* (15), 13492−13508.

(24) Makabenta, J. M. V.; Nabawy, A.; Li, C.-H.; Schmidt-Malan, S.; Patel, R.; Rotello, V. M. Nanomaterial-based therapeutics for antibiotic-resistant bacterial infections. *Nature Reviews Microbiology* **2021**, *19* (1), 23−36.

(25) Hochvaldová, L.; Večeřová, R.; Kolář, M.; Prucek, R.; Kvítek, L.; Lapčík, L.; Panáček, A. Antibacterial nanomaterials: Upcoming

hope to overcome antibiotic resistance crisis. *Nanotechnol. Rev.* **2022**, *11* (1), 1115−1142.

(26) Slavin, Y. N.; Asnis, J.; Häfeli, U. O.; Bach, H. Metal nanoparticles: Understanding the mechanisms behind antibacterial activity. *Journal of Nanobiotechnology* **2017**, *15*, No. 65, DOI: 10.1186/s12951-017-0308-z.

(27) Assa, F.; Jafarizadeh-Malmiri, H.; Ajamein, H.; Anarjan, N.; Vaghari, H.; Sayyar, Z.; Berenjian, A., A biotechnological perspective on the application of iron oxide nanoparticles. In *Nano Research*; Tsinghua University Press, 2016; Vol. *9*, pp 2203−2225.

(28) Lee, N. Y.; Ko, W. C.; Hsueh, P. R. Nanoparticles in the Treatment of Infections Caused by Multidrug-Resistant Organisms. *Front Pharmacol* **2019**, *10*, 1153.

(29) Gudkov, S. V.; Burmistrov, D. E.; Serov, D. A.; Rebezov, M. B.; Semenova, A. A.; Lisitsyn, A. B. Do Iron Oxide Nanoparticles Have Significant Antibacterial Properties? *Antibiotics* **2021**, *10* (7), 884.

(30) Arias, L. S.; Pessan, J. P.; Vieira, A. P. M.; De Lima, T. M. T.; Delbem, A. C. B.; Monteiro, D. R. Iron Oxide Nanoparticles for Biomedical Applications: A Perspective on Synthesis, Drugs, Antimicrobial Activity, and Toxicity. *Antibiotics* **2018**, *7* (2), 46.

(31) Ezealigo, U. S.; Ezealigo, B. N.; Aisida, S. O.; Ezema, F. I. Iron oxide nanoparticles in biological systems: Antibacterial and toxicology perspective. *JCIS Open* **2021**, *4*, No. 100027.

(32) Alprol, A. E.; Mansour, A. T.; Abdelwahab, A. M.; Ashour, M. Advances in Green Synthesis of Metal Oxide Nanoparticles by Marine Algae for Wastewater Treatment by Adsorption and Photocatalysis Techniques. *Catalysts* **2023**, *13* (5), 888.

(33) Tasnim, N. T.; Ferdous, N.; Rumon, M. M. H.; Shakil, M. S. The Promise of Metal-Doped Iron Oxide Nanoparticles as Antimicrobial Agent. *ACS Omega* **2024**, *9*, 16.

(34) Maglangit, F.; Yu, Y.; Deng, H. Bacterial pathogens: threat or treat (a review on bioactive natural products from bacterial pathogens). *Natural Product Reports* **2021**, *38* (4), 782−821.

(35) Janeway, C.; Travers, P.; Walport, M.; Shlomchik, M. J. *Immunobiology: the immune system in health and disease*; Garland Pub: New York, 2001; Vol. *2*.

(36) Peterson, J. W. Bacterial pathogenesis. *Medical Microbiology*, 4th ed.; University of Texas Medical Branch at Galveston, 1996.

(37) Silhavy, T. J.; Kahne, D.; Walker, S. The Bacterial Cell Envelope. *Cold Spring Harbor Perspectives in Biology* **2010**, *2* (5), No. a000414.

(38) Breijyeh, Z.; Jubeh, B.; Karaman, R. Resistance of gram-negative bacteria to current antibacterial agents and approaches to resolve it. *Molecules* **2020**, *25* (6), 1340.

(39) Zhang, H.; Niesel, D. W.; Peterson, J. W.; Klimpel, G. R. Lipoprotein Release by Bacteria: Potential Factor in Bacterial Pathogenesis. *Infect. Immun.* **1998**, *66* (11), 5196−5196.

(40) Bertics, P.; Gavala, M.; Denlinger, L. Endotoxins. In *Encyclopedia of Respiratory Medicine*; ScienceDirect, 2006; pp 80−85.

(41) Zhang, W.; Jiang, H.; Wu, G.; Huang, P.; Wang, H.; An, H.; Liu, S.; Zhang, W. The pathogenesis and potential therapeutic targets in sepsis. *MedComm* **2023**, *4* (6), No. e418.

(42) Ali, A.; Waris, A.; Khan, M. A.; Asim, M.; Khan, A. U.; Khan, S.; Zeb, J. Recent advancement, immune responses, and mechanism of action of various vaccines against intracellular bacterial infections. *Life Sciences* **2023**, *314*, No. 121332.

(43) Jurėnas, D.; Fraikin, N.; Goormaghtigh, F.; Van Melderen, L. Biology and evolution of bacterial toxin−antitoxin systems. *Nature Reviews Microbiology 2022 20:6* **2022**, *20* (6), 335−350.

(44) Smith, I. Mycobacterium tuberculosis Pathogenesis and Molecular Determinants of Virulence. *Clin. Microbiol. Rev.* **2003**, *16* (3), 463−463.

(45) Vollaard, A. M.; Verspaget, H. W.; Ali, S.; Visser, L. G.; Veenendaal, R. A.; Van Asten, H. A. G. H.; Widjaja, S.; Surjadi, C.; Van Dissel, J. T. Helicobacter pylori infection and typhoid fever in Jakarta, Indonesia. *Epidemiology and Infection* **2006**, *134* (1), 163−163.

(46) Sharma, A. K.; Dhasmana, N.; Dubey, N.; Kumar, N.; Gangwal, A.; Gupta, M.; Singh, Y. Bacterial Virulence Factors: Secreted for Survival. *Indian Journal of Microbiology* **2017**, *57* (1), 1−1.

(47) Belkaid, Y.; Hand, T. W. Role of the Microbiota in Immunity and inflammation. *Cell* **2014**, *157* (1), 121−121.

(48) Gerba, C. P. Environmentally Transmitted Pathogens. *Environmental Microbiology* **2009**, 445−445.

(49) C Reygaert, W. An overview of the antimicrobial resistance mechanisms of bacteria. *AIMS microbiology* **2018**, *4* (3), 482.

(50) Munita, J. M.; Arias, C. A., Mechanisms of Antibiotic Resistance. *Microbiology spectrum* **2016**, *4* (2). DOI: 10.1128/microbiolspec.VMBF-0016-2015

(51) Salazar-Alvarez, G., *Synthesis, characterisation and applications of iron oxide nanoparticles*, PhD Thesis, KTH: Sweden, 2004.

(52) Bock, D. C.; Tallman, K. R.; Guo, H.; Quilty, C.; Yan, S.; Smith, P. F.; Zhang, B.; Lutz, D. M.; McCarthy, A. H.; Huie, M. M.; Burnett, V.; Bruck, A. M.; Marschilok, A. C.; Takeuchi, E. S.; Liu, P.; Takeuchi, K. J. De)lithiation of spinel ferrites Fe3O4, MgFe2O4, and ZnFe2O4: A combined spectroscopic, diffraction and theory study. *Phys. Chem. Chem. Phys.* **2020**, *22* (45), 26200−26215.

(53) Jian, W.; Jia, R.; Wang, J.; Zhang, H. X.; Bai, F. Q. Iron oxides with a reverse spinel structure: Impact of active sites on molecule adsorption. *Inorganic Chemistry Frontiers* **2019**, *6* (10), 2810−2816.

(54) Sanchez-Lievanos, K. R.; Stair, J. L.; Knowles, K. E. Cation Distribution in Spinel Ferrite Nanocrystals: Characterization, Impact on their Physical Properties, and Opportunities for Synthetic Control. *Inorg. Chem.* **2021**, *60* (7), 4291−4305.

(55) Nagashima, M.; Ishida, T.; Akasaka, M. Distribution of Fe among octahedral sites and its effect on the crystal structure of pumpellyite. *Physics and Chemistry of Minerals* **2006**, *33* (3), 178−191.

(56) Wu, W.; He, Q.; Jiang, C. Magnetic Iron Oxide Nanoparticles: Synthesis and Surface Functionalization Strategies. *Nanoscale Research Letters* **2008**, *3* (11), 397−415.

(57) Bonvin, D.; Arakcheeva, A.; Millan, A.; Pinol, R.; Hofmann, H.; Mionic Ebersold, M. Controlling structural and magnetic properties of IONPs by aqueous synthesis for improved hyperthermia. *RSC Adv.* **2017**, *7* (22), 13159−13170.

(58) Wu, W.; Wu, Z.; Yu, T.; Jiang, C.; Kim, W.-S. Recent progress on magnetic iron oxide nanoparticles: synthesis, surface functional strategies and biomedical applications. *Sci. Technol. Adv. Mater.* **2015**, *16* (2), No. 023501.

(59) Bhushan, M.; Kumar, Y.; Periyasamy, L.; Viswanath, A. K. Antibacterial applications of α-Fe2O3/Co3O4 nanocomposites and study of their structural, optical, magnetic and cytotoxic characteristics. *Applied Nanoscience (Switzerland)* **2018**, *8* (1−2), 137−153.

(60) Clarke, D. M.; Marquina, C.; Lloyd, D. C.; Vallejo-Fernandez, G. Effect of the distribution of anisotropy constants on the magnetic properties of iron oxide nanoparticles. *J. Magn. Magn. Mater.* **2022**, *559*, 169543−169543.

(61) Estelrich, J.; Busquets, M. A. Iron Oxide Nanoparticles in Photothermal Therapy. *Molecules: A Journal of Synthetic Chemistry and Natural Product Chemistry* **2018**, *23* (7), 1567.

(62) Amendola, V.; Meneghetti, M.; Granozzi, G.; Agnoli, S.; Polizzi, S.; Riello, P.; Boscaini, A.; Anselmi, C.; Fracasso, G.; Colombatti, M.; Innocenti, C.; Gatteschi, D.; Sangregorio, C. Top-down synthesis of multifunctional iron oxide nanoparticles for macrophage labelling and manipulation. *J. Mater. Chem.* **2011**, *21* (11), 3803−3813.

(63) Abid, N.; Khan, A. M.; Shujait, S.; Chaudhary, K.; Ikram, M.; Imran, M.; Haider, J.; Khan, M.; Khan, Q.; Maqbool, M. Synthesis of nanomaterials using various top-down and bottom-up approaches, influencing factors, advantages, and disadvantages: A review. *Adv. Colloid Interface Sci.* **2022**, *300*, 102597−102597.

(64) Mahmud, N.; Anik, M. I.; Hossain, M. K.; Khan, M. I.; Uddin, S.; Ashrafuzzaman, M.; Rahaman, M. M. Advances in nanomaterial-based platforms to combat COVID-19: Diagnostics, preventions, therapeutics, and vaccine developments. *ACS Applied Bio Materials* **2022**, *5* (6), 2431−2460.

(65) Uddin, S.; Islam, M. R.; Chowdhury, M. R.; Wakabayashi, R.; Kamiya, N.; Moniruzzaman, M.; Goto, M. Lipid-based ionic-liquid-

mediated nanodispersions as biocompatible carriers for the enhanced transdermal delivery of a peptide drug. *ACS applied bio materials* **2021**, *4* (8), 6256−6267.

(66) Ansari, S. A.; Oves, M.; Satar, R.; Khan, A.; Ahmad, S. I.; Jafri, M. A.; Zaidi, S. K.; Alqahtani, M. H. Antibacterial activity of iron oxide nanoparticles synthesized by co-precipitation technology against Bacillus cereus and Klebsiella pneumoniae. *Polish Journal of Chemical Technology* **2017**, *19* (4), 110−115.

(67) Fexy, A. Structural Study on Iron Oxide Nanoparticles Prepared by Sol-Gel Method. *Int. J. Scientific Eng. Res.* **2018**, *9* (7), 324−329.

(68) Mehrabi, M.; Ghasemi, M. F.; Rasti, B.; Falahati, M.; Mirzaie, A.; Hasan, A. Nanoporous iron oxide nanoparticle: hydrothermal fabrication, human serum albumin interaction and potential antibacterial effects. *J. Biomol. Struct. Dyn.* **2021**, *39* (7), 2595−2606.

(69) Hooda, R.; Sharma, M. Green Synthesis, Characterization and Antibacterial Activity of Iron Oxide Nanoparticles. *Plant Archives* **2020**, *20* (1), 1196−1200.

(70) Yadav, V. K.; Ali, D.; Khan, S. H.; Gnanamoorthy, G.; Choudhary, N.; Yadav, K. K.; Thai, V. N.; Hussain, S. A.; Manhrdas, S. Synthesis and Characterization of Amorphous Iron Oxide Nanoparticles by the Sonochemical Method and Their Application for the Remediation of Heavy Metals from Wastewater. *Nanomaterials* **2020**, *10* (8), 1551.

(71) Omelchenko, A. I.; Sobol, E. N.; Simakin, A. V.; Serkov, A. A.; Sukhov, I. A.; Shafeev, G. A. Biofunctional magnetic 'core−shell' nanoparticles generated by laser ablation of iron in liquid. *Laser Physics* **2015**, *25* (2), 025607−025607.

(72) Hachani, R.; Lowdell, M.; Birchall, M.; Hervault, A.; Mertz, D.; Begin-Colin, S.; Thanh, N. T. B. D. K. Polyol synthesis, functionalisation, and biocompatibility studies of superparamagnetic iron oxide nanoparticles as potential MRI contrast agents. *Nanoscale* **2016**, *8* (6), 3278−3287.

(73) Kekalo, K.; Koo, K.; Zeitchick, E.; Baker, I. Microemulsion Synthesis of Iron Core/Iron Oxide Shell Magnetic Nanoparticles and Their Physicochemical Properties. *Materials Research Society symposia proceedings. Materials Research Society* **2012**, *1416*, 61−66.

(74) Islam, M. R.; Uddin, S.; Chowdhury, M. R.; Wakabayashi, R.; Moniruzzaman, M.; Goto, M. Insulin transdermal delivery system for diabetes treatment using a biocompatible ionic liquid-based microemulsion. *ACS Appl. Mater. Interfaces* **2021**, *13* (36), 42461−42472.

(75) Uddin, S.; Islam, M. R.; Moshikur, R. M.; Wakabayashi, R.; Moniruzzaman, M.; Goto, M. Modification with Conventional Surfactants to Improve a Lipid-Based Ionic-Liquid-Associated Transcutaneous Anticancer Vaccine. *Molecules* **2023**, *28* (7), 2969.

(76) Raghunath, A.; Perumal, E. Metal oxide nanoparticles as antimicrobial agents: a promise for the future. *International journal of antimicrobial agents* **2017**, *49* (2), 137−152.

(77) Ali, A.; Zafar, H.; Zia, M.; ul Haq, I.; Phull, A. R.; Ali, J. S.; Hussain, A. Synthesis, characterization, applications, and challenges of iron oxide nanoparticles. *Nanotechnology, science and applications* **2016**, *9*, 49−67.

(78) Zhang, J.; Zhang, T.; Gao, J. Biocompatible iron oxide nanoparticles for targeted cancer gene therapy: A review. *Nanomaterials* **2022**, *12* (19), 3323.

(79) Uddin, S.; Chowdhury, M. R.; Wakabayashi, R.; Kamiya, N.; Moniruzzaman, M.; Goto, M. Lipid based biocompatible ionic liquids: synthesis, characterization and biocompatibility evaluation. *Chem. Commun.* **2020**, *56* (89), 13756−13759.

(80) Patil, S.; Mishra, V. S.; Reddy, P. C.; Lochab, B. Multifunctional Multicomponent Highly Biocompatible pH-Responsive Iron-Oxide Embedded Nanodiamond Cargo for Artesunate to Inhibit Cancer Growth. *ACS Materials Letters* **2023**, *5* (2), 336−340.

(81) Kannan, D.; Yadav, N.; Ahmad, S.; Namdev, P.; Bhattacharjee, S.; Lochab, B.; Singh, S. Pre-clinical study of iron oxide nanoparticles fortified artesunate for efficient targeting of malarial parasite. *EBioMedicine* **2019**, *45*, 261−277.

(82) Guo, H.; Barnard, A. S. Naturally occurring iron oxide nanoparticles: morphology, surface chemistry and environmental stability. *Journal of Materials Chemistry A* **2013**, *1* (1), 27−42.

(83) Nasiri, K.; Masoumi, S. M.; Amini, S.; Goudarzi, M.; Tafreshi, S. M.; Bagheri, A.; Yasamineh, S.; Alwan, M.; Arellano, M. T. C.; Gholizadeh, O. Recent advances in metal nanoparticles to treat periodontitis. *J. Nanobiotechnol.* **2023**, *21* (1), 283.

(84) Ajinkya, N.; Yu, X.; Kaithal, P.; Luo, H.; Somani, P.; Ramakrishna, S. Magnetic iron oxide nanoparticle (IONP) synthesis to applications: present and future. *Materials* **2020**, *13* (20), 4644.

(85) Singh, J.; Dutta, T.; Kim, K. H.; Rawat, M.; Samddar, P.; Kumar, P. 'Green' synthesis of metals and their oxide nanoparticles: applications for environmental remediation. *J. Nanobiotechnology* **2018**, *16* (1), 84.

(86) Miranda, A.; Akpobolokemi, T.; Chung, E.; Ren, G.; Raimi-Abraham, B. T. pH Alteration in Plant-Mediated Green Synthesis and Its Resultant Impact on Antimicrobial Properties of Silver Nanoparticles (AgNPs). *Antibiotics (Basel)* **2022**, *11* (11), 1592.

(87) Sharaf, M.; Sewid, A. H.; Hamouda, H. I.; Elharrif, M. G.; El-Demerdash, A. S.; Alharthi, A.; Hashim, N.; Hamad, A. A.; Selim, S.; Alkhalifah, D. H. M.; Hozzein, W. N.; Abdalla, M.; Saber, T. Rhamnolipid-Coated Iron Oxide Nanoparticles as a Novel Multitarget Candidate against Major Foodborne E. coli Serotypes and Methicillin-Resistant S. aureus. *Microbiology Spectrum* **2022**, *10* (4), No. e00250-22.

(88) Ismail, A. S.; Mady, A. H.; Tawfik, S. M. Synthesis, Characterization and Biological Activity of Iron (III) Oxide and Titanium (IV) Oxide Nanoparticle Dispersed Polyester Resin Nanocomposites. *Arabian Journal for Science and Engineering* **2020**, *45* (1), 197−203.

(89) Khalid, H. F.; Tehseen, B.; Sarwar, Y.; Hussain, S. Z.; Khan, W. S.; Raza, Z. A.; Bajwa, S. Z.; Kanaras, A. G.; Hussain, I.; Rehman, A. Biosurfactant coated silver and iron oxide nanoparticles with enhanced anti-biofilm and anti-adhesive properties. *Journal of Hazardous Materials* **2019**, *364*, 441−448.

(90) Moshafi, M. H.; Ranjbar, M.; Ilbeigi, G. Biotemplate of albumen for synthesized iron oxide quantum dots nanoparticles (QDNPs) and investigation of antibacterial effect against pathogenic microbial strains. *Int. J. Nanomed.* **2019**, *14*, 3273−3282.

(91) Abdulhady, Y. A. M.; El-Shazly, M. M.; El-Kased, R. F. Evaluation of antibacterial activity and toxic metal removal of chemically synthesized magnetic iron oxide titanium coated nanoparticles and application in bacterial treatment. *Journal of Environmental Science and Health - Part A Toxic/Hazardous Substances and Environmental Engineering* **2018**, *53* (3), 205−212.

(92) Taylor, E. N.; Kummer, K. M.; Durmus, N. G.; Leuba, K.; Tarquinio, K. M.; Webster, T. J. Superparamagnetic iron oxide nanoparticles (SPION) for the treatment of antibiotic-resistant biofilms. *Small* **2012**, *8* (19), 3016−3027.

(93) Abdulsada, F. M.; Hussein, N. N.; Sulaiman, G. M.; Al Ali, A.; Alhujaily, M. Evaluation of the Antibacterial Properties of Iron Oxide, Polyethylene Glycol, and Gentamicin Conjugated Nanoparticles against Some Multidrug-Resistant Bacteria. *Journal of Functional Biomaterials* **2022**, *13* (3), 138.

(94) Armenia, I.; Marcone, G. L.; Berini, F.; Orlandi, V. T.; Pirrone, C.; Martegani, E.; Gornati, R.; Bernardini, G.; Marinelli, F., Magnetic nanoconjugated teicoplanin: A novel tool for bacterial infection site targeting. *Frontiers in Microbiology* **2018**, *9* (OCT). DOI: 10.3389/fmicb.2018.02270

(95) Gabrielyan, L.; Hovhannisyan, A.; Gevorgyan, V.; Ananyan, M.; Trchounian, A. Antibacterial effects of iron oxide (Fe 3 O 4) nanoparticles: distinguishing concentration-dependent effects with different bacterial cells growth and membrane-associated mechanisms. *Appl. Microbiol. Biotechnol.* **2019**, *103* (6), 2773−2782.

(96) Arokiyaraj, S.; Saravanan, M.; Udaya Prakash, N. K.; Valan Arasu, M.; Vijayakumar, B.; Vincent, S. Enhanced antibacterial activity of iron oxide magnetic nanoparticles treated with Argemone mexicana L. leaf extract: An in vitro study. *Mater. Res. Bull.* **2013**, *48* (9), 3323−3327.

(97) Arshad, M.; Alyousef, A.; Ahmad, I.; Khan, J. M.; Shahzad, S. A., Low temperature synthesis of superparamagnetic iron oxide (Fe3O4) nanoparticles and their ROS mediated inhibition of biofilm formed by food-associated bacteria. *Frontiers in Microbiology* **2018**, *9* (). DOI: 10.3389/fmicb.2018.02567

(98) Bhattacharya, P.; Neogi, S. Gentamicin coated iron oxide nanoparticles as novel antibacterial agents. *Materials Research Express* **2017**, *4* (9), No. 095005.

(99) Prabhu, Y. T.; Rao, K. V.; Kumari, B. S.; Kumar, V. S. S.; Pavani, T. Synthesis of Fe3O4 nanoparticles and its antibacterial application. *International Nano Letters* **2015**, *5* (2), 85–92.

(100) Philip, S.; Kuriakose, S. Studies on the antibacterial activity of water-soluble iron oxide nanoparticle- β-cyclodextrin aggregates against selected human pathogenic bacteria. *Nano-Structures and Nano-Objects* **2018**, *16*, 347–353.

(101) Khan, S.; Shah, Z. H.; Riaz, S.; Ahmad, N.; Islam, S.; Raza, M. A.; Naseem, S. Antimicrobial activity of citric acid functionalized iron oxide nanoparticles − Superparamagnetic effect. *Ceram. Int.* **2020**, *46* (8), 10942–10951.

(102) Brahmbhatt, P. N.; Bharucha, S. R.; Bhatt, A.; Dave, M. S. The Synthesis, Characterization, and Antimicrobial Activity of Magnetite (Fe3O4) Nanoparticles by the Sol−Gel Method. *Eng. Proc.* **2023**, *56* (1), 293.

(103) Ismail, R. A.; Sulaiman, G. M.; Abdulrahman, S. A.; Marzoog, T. R. Antibacterial activity of magnetic iron oxide nanoparticles synthesized by laser ablation in liquid. *Materials Science and Engineering: C* **2015**, *53*, 286–297.

(104) Arias, L. S.; Pessan, J. P.; Vieira, A. P. M.; Lima, T. M. T. d.; Delbem, A. C. B.; Monteiro, D. R. Iron oxide nanoparticles for biomedical applications: a perspective on synthesis, drugs, antimicrobial activity, and toxicity. *Antibiotics* **2018**, *7* (2), 46.

(105) Arakha, M.; Pal, S.; Samantarrai, D.; Panigrahi, T. K.; Mallick, B. C.; Pramanik, K.; Mallick, B.; Jha, S. Antimicrobial activity of iron oxide nanoparticle upon modulation of nanoparticle-bacteria interface. *Sci. Rep.* **2015**, *5* (1), No. 14813.

(106) Ling, W.; Wang, M.; Xiong, C.; Xie, D.; Chen, Q.; Chu, X.; Qiu, X.; Li, Y.; Xiao, X. Synthesis, surface modification, and applications of magnetic iron oxide nanoparticles. *J. Mater. Res.* **2019**, *34* (11), 1828–1844.

(107) Swoboda, J. G.; Campbell, J.; Meredith, T. C.; Walker, S. Wall Teichoic Acid Function, Biosynthesis, and Inhibition. *Chembiochem: a European journal of chemical biology* **2010**, *11* (1), 35–35.

(108) de Lacerda Coriolano, D.; de Souza, J. B.; Bueno, E. V.; Medeiros, S. M. d. F. R. d. S.; Cavalcanti, I. D. L.; Cavalcanti, I. M. F. Antibacterial and antibiofilm potential of silver nanoparticles against antibiotic-sensitive and multidrug-resistant Pseudomonas aeruginosa strains. *Brazilian Journal of Microbiology* **2021**, *52*, 267–278.

(109) Azam, A.; Ahmed, A. S.; Oves, M.; Khan, M. S.; Habib, S. S.; Memic, A. Antimicrobial activity of metal oxide nanoparticles against Gram-positive and Gram-negative bacteria: a comparative study. *International journal of nanomedicine* **2012**, 6003–6009.

(110) Nakai, K.; Tsuruta, D. What are reactive oxygen species, free radicals, and oxidative stress in skin diseases? *International journal of molecular sciences* **2021**, *22* (19), 10799.

(111) Ray, P. D.; Huang, B.-W.; Tsuji, Y. Reactive oxygen species (ROS) homeostasis and redox regulation in cellular signaling. *Cellular signalling* **2012**, *24* (5), 981–990.

(112) Wydra, R. J.; Oliver, C. E.; Anderson, K. W.; Dziubla, T. D.; Hilt, J. Z. Accelerated generation of free radicals by iron oxide nanoparticles in the presence of an alternating magnetic field. *RSC Adv.* **2015**, *5* (24), 18888–18893.

(113) Kiggundu, R.; Lusaya, E.; Seni, J.; Waswa, J. P.; Kakooza, F.; Tjipura, D.; Kikule, K.; Muiva, C.; Joshi, M. P.; Stergachis, A.; Kitutu, F. E.; Konduri, N. Identifying and addressing challenges to antimicrobial use surveillance in the human health sector in low- and middle-income countries: experiences and lessons learned from Tanzania and Uganda. *Antimicrobial Resistance and Infection Control* **2023**, *12* (1), 1–8.

(114) Abdal Dayem, A.; Hossain, M.; Lee, S.; Kim, K.; Saha, S.; Yang, G.-M.; Choi, H.; Cho, S.-G. The Role of Reactive Oxygen Species (ROS) in the Biological Activities of Metallic Nanoparticles. *International Journal of Molecular Sciences* **2017**, *18* (1), 120.

(115) Kaushik, A.; Khan, R.; Solanki, P. R.; Pandey, P.; Alam, J.; Ahmad, S.; Malhotra, B. D. Iron oxide nanoparticles−chitosan composite based glucose biosensor. *Biosens. Bioelectron.* **2008**, *24* (4), 676−683.

(116) Chatterjee, S.; Bandyopadhyay, A.; Sarkar, K. Effect of iron oxide and gold nanoparticles on bacterial growth leading towards biological application. *J. Nanobiotechnol.* **2011**, *9* (1), 1–7.

(117) Current, K. M.; Dissanayake, N. M.; Obare, S. O. Effect of Iron Oxide Nanoparticles and Amoxicillin on Bacterial Growth in the Presence of Dissolved Organic Carbon. *Biomedicines 2017, Vol. 5, Page 55* **2017**, *5* (3), 55–55.

(118) Liu, X.; Ma, Z.; Xing, J.; Liu, H. Preparation and characterization of amino−silane modified superparamagnetic silica nanospheres. *J. Magn. Magn. Mater.* **2004**, *270* (1−2), 1−6.

(119) Yilmaz, E.; Soylak, M., Functionalized nanomaterials for sample preparation methods. In *Handbook of Nanomaterials in analytical chemistry*; Elsevier: 2020; pp 375−413.

(120) Riaz, S.; Bashir, M.; Naseem, S. Iron Oxide Nanoparticles Prepared by Modified Co-Precipitation Method. *IEEE Trans. Magn.* **2014**, *50* (1), 1–4.

(121) Pallela, P. N. V. K.; Ummey, S.; Ruddaraju, L. K.; Gadi, S.; Cherukuri, C. S. L.; Barla, S.; Pammi, S. V. N. Antibacterial efficacy of green synthesized α-Fe2O3 nanoparticles using Sida cordifolia plant extract. *Heliyon* **2019**, *5* (11), No. e02765.

(122) Rufus, A.; Sreeju, N.; Philip, D. Synthesis of biogenic hematite (α-Fe2O3) nanoparticles for antibacterial and nanofluid applications. *RSC Adv.* **2016**, *6* (96), 94206−94217.

(123) Patra, J. K.; Baek, K. H. Green biosynthesis of magnetic iron oxide (Fe3O4) nanoparticles using the aqueous extracts of food processing wastes under photo-catalyzed condition and investigation of their antimicrobial and antioxidant activity. *Journal of Photochemistry and Photobiology B: Biology* **2017**, *173*, 291−300.

(124) Toropova, Y. G.; Zelinskaya, I. A.; Gorshkova, M. N.; Motorina, D. S.; Korolev, D. V.; Velikonivtsev, F. S.; Gareev, K. G. Albumin covering maintains endothelial function upon magnetic iron oxide nanoparticles intravenous injection in rats. *J. Biomed. Mater. Res., Part A* **2021**, *109* (10), 2017−2026.

(125) Sathishkumar, G.; Logeshwaran, V.; Sarathbabu, S.; Jha, P. K.; Jeyaraj, M.; Rajkuberan, C.; Senthilkumar, N.; Sivaramakrishnan, S. Green synthesis of magnetic Fe3O4 nanoparticles using Couroupita guianensis Aubl. fruit extract for their antibacterial and cytotoxicity activities. *Taylor & Francis* **2018**, *46* (3), 589−598.

(126) Huq, M. A.; Ashrafudoulla, M.; Rahman, M. M.; Balusamy, S. R.; Akter, S. Green synthesis and potential antibacterial applications of bioactive silver nanoparticles: A review. *Polymers* **2022**, *14* (4), 742.

(127) Ghosh, A.; Das, B. K.; Roy, A.; Mandal, B.; Chandra, G. Antibacterial activity of some medicinal plant extracts. *Journal of natural medicines* **2008**, *62*, 259−262.

(128) Alaiya, M. A.; Odeniyi, M. A. Utilisation of Mangifera indica plant extracts and parts in antimicrobial formulations and as a pharmaceutical excipient: a review. *Future Journal of Pharmaceutical Sciences* **2023**, *9* (1), 29.

(129) Khan, A.; Vishvakarma, R.; Sharma, P.; Sharma, S.; Vimal, A., Green Synthesis of Metal-Oxide Nanoparticles from Fruits and Their Waste Materials for Diverse Applications. In *Nanomaterials from Agricultural and Horticultural Products*; Springer: 2023; pp 81−119.

(130) Longmire, M.; Choyke, P. L.; Kobayashi, H. Clearance properties of nano-sized particles and molecules as imaging agents: considerations and caveats. *Nanomedicine* **2008**, *3*, 703.

(131) Hammad, E. N.; Salem, S. S.; Mohamed, A. A.; El-Dougdoug, W. Environmental Impacts of Ecofriendly Iron Oxide Nanoparticles on Dyes Removal and Antibacterial Activity. *Appl. Biochem. Biotechnol.* **2022**, *194* (12), 6053−6067.

(132) Wang, G.; Liu, Z.; Lin, R.; Li, E.; Mao, Z.; Ling, J.; Yang, Y.; Yin, W.-B.; Xie, B. Biosynthesis of Antibiotic Leucinostatins in Bio-

control Fungus Purpureocillium lilacinum and Their Inhibition on Phytophthora Revealed by Genome Mining. *PLOS Pathogens* **2016**, *12* (7), No. e1005685.

(133) Montemartini Corte, A.; Liotta, M.; Venturi, C. B.; Calegari, L. Antibacterial activity of Penicillium spp. strains isolated in extreme environments. *Polar Biology* **2000**, *23* (4), 294−297.

(134) Al-Aamri, M. S.; Al-Abousi, N. M.; Al-Jabri, S. S.; Alam, T.; Khan, S. A. Chemical composition and in-vitro antioxidant and antimicrobial activity of the essential oil of Citrus aurantifolia L. leaves grown in Eastern Oman. *J. Taibah Univ Med. Sci.* **2018**, *13* (2), 108−112.

(135) Al-Otibi, F.; Moria, G. A.; Alharbi, R. I.; Yassin, M. T.; Al-Askar, A. A. The Antifungal Properties of Tamarix aphylla Extract against Some Plant Pathogenic Fungi. *Microorganisms* **2023**, *11* (1), 127.

(136) Haroun, M. F.; Al-Kayali, R. S. Synergistic effect of Thymbra spicata L. extracts with antibiotics against multidrug- resistant Staphylococcus aureus and Klebsiella pneumoniae strains. *Iranian Journal of Basic Medical Sciences* **2016**, *19* (11), 1193−1200.

(137) a. K. v.. Antimicrobial activity of Lawsonia inermis leaf extracts against some human pathogens. *International Journal of Current Microbiology and Applied Sciences* **2013**, *2* (5), 342−349.

(138) Naseer, S.; Hussain, S.; Naeem, N.; Pervaiz, M.; Rahman, M., The phytochemistry and medicinal value of Psidium guajava (guava). *Clinical Phytoscience* **2018**, *4* (1). DOI: 10.1186/s40816-018-0093-8

(139) Zakariya, N. A.; Majeed, S.; Jusof, W. H. W. Investigation of antioxidant and antibacterial activity of iron oxide nanoparticles (IONPS) synthesized from the aqueous extract of Penicillium spp. *Sensors International* **2022**, *3*, 100164.

(140) Mohandoss, N.; Renganathan, S.; Subramaniyan, V.; Nagarajan, P.; Elavarasan, V.; Subramaniyan, P.; Vijayakumar, S. Investigation of Biofabricated Iron Oxide Nanoparticles for Antimicrobial and Anticancer Efficiencies. *Applied Sciences (Switzerland)* **2022**, *12* (24), 12986.

(141) Ahmad, W.; Khan, A. U.; Shams, S.; Qin, L.; Yuan, Q.; Ahmad, A.; Wei, Y.; Khan, Z. U. H.; Ullah, S.; Rahman, A. U. Eco-benign approach to synthesize spherical iron oxide nanoparticles: A new insight in photocatalytic and biomedical applications. *Journal of Photochemistry and Photobiology B: Biology* **2020**, *205*, 111821.

(142) Erci, F.; Cakir-Koc, R. Rapid green synthesis of noncytotoxic iron oxide nanoparticles using aqueous leaf extract of Thymbra spicata and evaluation of their antibacterial, antibiofilm, and antioxidant activity. *Inorganic and Nano-Metal Chemistry* **2021**, *51* (5), 683−692.

(143) Chauhan, S.; Upadhyay, L. S. B. Biosynthesis of iron oxide nanoparticles using plant derivatives of Lawsonia inermis (Henna) and its surface modification for biomedical application. *Nanotechnology for Environmental Engineering* **2019**, *4* (1), No. 8, DOI: 10.1007/s41204-019-0055-5.

(144) Madubuonu, N.; Aisida, S. O.; Ali, A.; Ahmad, I.; Zhao, T. k.; Botha, S.; Maaza, M.; Ezema, F. I. Biosynthesis of iron oxide nanoparticles via a composite of Psidium guavaja-Moringa oleifera and their antibacterial and photocatalytic study. *Journal of Photochemistry and Photobiology B: Biology* **2019**, *199*, 111601.

(145) Ramalingam, V.; Dhinesh, P.; Sundaramahalingam, S.; Rajaram, R. Green fabrication of iron oxide nanoparticles using grey mangrove Avicennia marina for antibiofilm activity and in vitro toxicity. *Surfaces and Interfaces* **2019**, *15*, 70−77.

(146) Patra, J. K.; Ali, M. S.; Oh, I. G.; Baek, K. H. Proteasome inhibitory, antioxidant, and synergistic antibacterial and anticandidal activity of green biosynthesized magnetic Fe3O4 nanoparticles using the aqueous extract of corn (Zea mays L.) ear leaves. *Artificial Cells, Nanomedicine and Biotechnology* **2017**, *45* (2), 349−356.

(147) Bao, N.; Gupta, A. Self-assembly of superparamagnetic nanoparticles. *J. Mater. Res.* **2011**, *26* (2), 111−121.

(148) Bustamante-Torres, M.; Romero-Fierro, D.; Estrella-Nuñez, J.; Arcentales-Vera, B.; Chichande-Proaño, E.; Bucio, E. Polymeric composite of magnetite iron oxide nanoparticles and their application in biomedicine: a review. *Polymers* **2022**, *14* (4), 752.

(149) Zúñiga-Miranda, J.; Guerra, J.; Mueller, A.; Mayorga-Ramos, A.; Carrera-Pacheco, S. E.; Barba-Ostria, C.; Heredia-Moya, J.; Guamán, L. P. Iron oxide nanoparticles: green synthesis and their antimicrobial activity. *Nanomaterials* **2023**, *13* (22), 2919.

(150) Xie, W.; Guo, Z.; Gao, F.; Gao, Q.; Wang, D.; Liaw, B. S.; Cai, Q.; Sun, X.; Wang, X.; Zhao, L. Shape-, size- and structure-controlled synthesis and biocompatibility of iron oxide nanoparticles for magnetic theranostics. *Theranostics* **2018**, *8* (12), 3284−3284.

(151) Tharani, K.; Jegatha Christy, A.; Sagadevan, S.; Nehru, L. C. Photocatalytic and antibacterial performance of iron oxide nanoparticles formed by the combustion method. *Chem. Phys. Lett.* **2021**, *771*, 138524−138524.

(152) De Jong, W. H.; Borm, P. J. A. Drug delivery and nanoparticles: Applications and hazards. *Int. J. Nanomed.* **2008**, *3* (2), 133−133.

(153) Rizvi, S. A. A.; Saleh, A. M. Applications of nanoparticle systems in drug delivery technology. *Saudi Pharmaceutical Journal: SPJ.* **2018**, *26* (1), 64−64.

(154) Stephen Inbaraj, B.; Tsai, T. Y.; Chen, B. H. Synthesis, characterization and antibacterial activity of superparamagnetic nanoparticles modified with glycol chitosan. *Science and Technology of Advanced Materials* **2012**, *13* (1), 015002.

(155) Zhou, Y.; Kumon, R. E.; Cui, J.; Deng, C. X. The Size of Sonoporation Pores on the Cell Membrane. *Ultrasound in Medicine & Biology* **2009**, *35* (10), 1756−1760.

(156) Barrow, M.; Taylor, A.; Fuentes-Caparrós, A. M.; Sharkey, J.; Daniels, L. M.; Mandal, P.; Park, B. K.; Murray, P.; Rosseinsky, M. J.; Adams, D. J. SPIONs for cell labelling and tracking using MRI: magnetite or maghemite? *Biomaterials science* **2018**, *6* (1), 101−106.

(157) Mahmoudi, M.; Sahraian, M. A.; Shokrgozar, M. A.; Laurent, S. Superparamagnetic iron oxide nanoparticles: promises for diagnosis and treatment of multiple sclerosis. *ACS chemical neuroscience* **2011**, *2* (3), 118−140.

(158) Feng, Q.; Liu, Y.; Huang, J.; Chen, K.; Huang, J.; Xiao, K. Uptake, distribution, clearance, and toxicity of iron oxide nanoparticles with different sizes and coatings. *Sci. Rep.* **2018**, *8* (1), 1−13.

(159) Tong, S.; Quinto, C. A.; Zhang, L.; Mohindra, P.; Bao, G. Size-dependent heating of magnetic iron oxide nanoparticles. *ACS Nano* **2017**, *11* (7), 6808−6816.

(160) Freis, B.; Ramirez, M. D. L. A.; Kiefer, C.; Harlepp, S.; Iacovita, C.; Henoumont, C.; Affolter-Zbaraszczuk, C.; Meyer, F.; Mertz, D.; Boos, A.; et al. Effect of the Size and Shape of Dendronized Iron Oxide Nanoparticles Bearing a Targeting Ligand on MRI, Magnetic Hyperthermia, and Photothermia Properties—From Suspension to In Vitro Studies. *Pharmaceutics* **2023**, *15* (4), 1104.

(161) Shineh, G.; Mobaraki, M.; Afzali, E.; Alakija, F.; Velisdeh, Z. J.; Mills, D. K. Antimicrobial Metal and Metal Oxide Nanoparticles in Bone Tissue Repair. *Biomedical Materials & Devices* **2024**, *2*, 918.

(162) Aadinath, W.; Muthuvijayan, V. Antibacterial and angiogenic potential of iron oxide nanoparticles-stabilized acrylate-based scaffolds for bone tissue engineering applications. *Colloids Surf., B* **2023**, *231*, No. 113572.

(163) Vahini, M.; Rakesh, S. S.; Subashini, R.; Loganathan, S.; Prakash, D. G. In vitro biological assessment of green synthesized iron oxide nanoparticles using Anastatica hierochuntica (Rose of Jericho). *Biomass Conversion and Biorefinery* **2023**, 1−11.

(164) Uniyal, S.; Choudhary, K.; Sachdev, S.; Kumar, S. Nano-bio fusion: Advancing biomedical applications and biosensing with functional nanomaterials. *Optics & Laser Technology* **2024**, *168*, No. 109938.

(165) Ioncica, M.-C.; Bandyopadhyay, S.; Bali, N.; Socoliuc, V.; Bernad, S. I. Investigation of Cubic and Spherical IONPs' Rheological Characteristics and Aggregation Patterns from the Perspective of Magnetic Targeting. *Magnetochemistry* **2023**, *9* (4), 99.

(166) Shahbazi, F.; Ahmadi, R.; Noghani, M.; Karimi, G. Antibacterial activity of the Iron-Zinc Oxide nanoparticles synthesized via electric discharge method. *International Journal of Nano Dimension* **2023**, *14* (1), 60−72.

(167) Sayed, F. A.; Eissa, N. G.; Shen, Y.; Hunstad, D. A.; Wooley, K. L.; Elsabahy, M. Morphologic design of nanostructures for enhanced antimicrobial activity. *J. Nanobiotechnology* **2022**, *20* (1), 536.

(168) Augustine, R.; Hasan, A.; Primavera, R.; Wilson, R. J.; Thakor, A. S.; Kevadiya, B. D. Cellular uptake and retention of nanoparticles: Insights on particle properties and interaction with cellular components. *Materials Today Communications* **2020**, *25*, No. 101692.

(169) Song, Y.; Elsabahy, M.; Collins, C. A.; Khan, S.; Li, R.; Hreha, T. N.; Shen, Y.; Lin, Y.-N.; Letteri, R. A.; Su, L.; et al. Morphologic design of silver-bearing sugar-based polymer nanoparticles for uroepithelial cell binding and antimicrobial delivery. *Nano Lett.* **2021**, *21* (12), 4990−4998.

(170) Elsabahy, M.; Song, Y.; Eissa, N. G.; Khan, S.; Hamad, M. A.; Wooley, K. L. Morphologic design of sugar-based polymer nanoparticles for delivery of antidiabetic peptides. *J. Controlled Release* **2021**, *334*, 1−10.

(171) Cheon, J. Y.; Kim, S. J.; Rhee, Y. H.; Kwon, O. H.; Park, W. H. Shape-dependent antimicrobial activities of silver nanoparticles. *International journal of nanomedicine* **2019**, *14*, 2773−2780.

(172) Das, S.; Diyali, S.; Vinothini, G.; Perumalsamy, B.; Balakrishnan, G.; Ramasamy, T.; Dharumadurai, D.; Biswas, B. Synthesis, morphological analysis, antibacterial activity of iron oxide nanoparticles and the cytotoxic effect on lung cancer cell line. *Heliyon* **2020**, *6* (9), No. e04953.

(173) Carmo, P. H. F. D.; Garcia, M. T.; Figueiredo-Godoi, L. M. A.; Lage, A. C. P.; Silva, N. S. D.; Junqueira, J. C. Metal Nanoparticles to Combat Candida albicans Infections: An Update. *Microorganisms* **2023**, *11* (1), 138.

(174) Yu, B.; Wang, Z.; Almutairi, L.; Huang, S.; Kim, M.-H. Harnessing iron-oxide nanoparticles towards the improved bactericidal activity of macrophage against Staphylococcus aureus. *Nanomedicine: Nanotechnology, Biology and Medicine* **2020**, *24*, No. 102158.

(175) Lal, N.; Seifan, M.; Ebrahiminezhad, A.; Berenjian, A. The Effect of Iron Oxide Nanoparticles on the Menaquinone-7 Isomer Composition and Synthesis of the Biologically Significant All-Trans Isomer. *Nanomaterials* **2023**, *13* (12), 1825.

(176) Xie, W.; Guo, Z.; Gao, F.; Gao, Q.; Wang, D.; Liaw, B.-S.; Cai, Q.; Sun, X.; Wang, X.; Zhao, L. Shape-, size- and structure-controlled synthesis and biocompatibility of iron oxide nanoparticles for magnetic theranostics. *Theranostics* **2018**, *8* (12), 3284−3307.

(177) Le Ouay, B.; Stellacci, F. Antibacterial activity of silver nanoparticles: A surface science insight. *Nano today* **2015**, *10* (3), 339−354.

(178) Agarwal, H.; Nakara, A.; Shanmugam, V. K. Anti-inflammatory mechanism of various metal and metal oxide nanoparticles synthesized using plant extracts: A review. *Biomedicine & Pharmacotherapy* **2019**, *109*, 2561−2572.

(179) Waghchaure, R. H.; Adole, V. A. Biosynthesis of metal and metal oxide nanoparticles using various parts of plants for antibacterial, antifungal and anticancer activity: A review. *Journal of the Indian Chemical Society* **2023**, *100*, No. 100987.

(180) Gautam, S.; Bansal, D.; Bhatnagar, D.; Sharma, C.; Goyal, N., Synthesis of iron-based nanoparticles by chemical methods and their biomedical applications. In *Oxides for Medical Applications*; Elsevier, 2023; pp 167−195.

(181) Chang, H.; Kim, B. H.; Lim, S. G.; Baek, H.; Park, J.; Hyeon, T. Role of the precursor composition in the synthesis of metal ferrite nanoparticles. *Inorg. Chem.* **2021**, *60* (7), 4261−4268.

(182) Sharifi Dehsari, H.; Halda Ribeiro, A.; Ersoz, B.; Tremel, W.; Jakob, G.; Asadi, K. Effect of precursor concentration on size evolution of iron oxide nanoparticles. *CrystEngComm* **2017**, *19* (44), 6694−6702.

(183) Wang, G.; Cui, M.; Qiu, Y.; Miao, Y.; Ma, H.; Zhang, H.; Zhang, Y.; Liu, X.; Yi, J.; Peng, M.; et al. FeCO3 as a novel precursor for controllable synthesis of monodisperse iron oxide nanoparticles via solution thermal decomposition. *Micro & Nano Letters* **2021**, *16* (11), 552−557.

(184) Thakur, A.; Kumar, A.; Kaya, S.; Marzouki, R.; Zhang, F.; Guo, L. Recent Advancements in Surface Modification, Characterization and Functionalization for Enhancing the Biocompatibility and Corrosion Resistance of Biomedical Implants. *Coatings* **2022**, *12* (10), 1459.

(185) Zhu, N.; Ji, H.; Yu, P.; Niu, J.; Farooq, M.; Akram, M. W.; Udego, I.; Li, H.; Niu, X. Surface modification of magnetic iron oxide nanoparticles. *Nanomaterials* **2018**, *8* (10), 810.

(186) Abd Elrahman, A. A.; Mansour, F. R. Targeted magnetic iron oxide nanoparticles: Preparation, functionalization and biomedical application. *Journal of Drug Delivery Science and Technology* **2019**, *52*, 702−712.

(187) Abakumov, M. A.; Semkina, A. S.; Skorikov, A. S.; Vishnevskiy, D. A.; Ivanova, A. V.; Mironova, E.; Davydova, G. A.; Majouga, A. G.; Chekhonin, V. P. Toxicity of iron oxide nanoparticles: Size and coating effects. *Journal of Biochemical and Molecular Toxicology* **2018**, *32* (12), e22225−e22225.

(188) Anush, K.; Shushanik, K.; Susanna, T.; Ashkhen, H. Antibacterial effect of silver and iron oxide nanoparticles in combination with antibiotics on E. coli K12. *BioNanoScience* **2019**, *9*, 587−596.

(189) Khashan, K. S.; Sulaiman, G. M.; Mahdi, R. Preparation of iron oxide nanoparticles-decorated carbon nanotube using laser ablation in liquid and their antimicrobial activity. *Artificial cells, nanomedicine, and biotechnology, Taylor & Francis* **2017**, *45* (8), 1699−1709.

(190) Gabrielyan, L.; Badalyan, H.; Gevorgyan, V.; Trchounian, A. Comparable antibacterial effects and action mechanisms of silver and iron oxide nanoparticles on Escherichia coli and Salmonella typhimurium. *Scientific Reports* **2020**, *10* (1), 1−12.

(191) Lee, C. M.; Jeong, H. J.; Kim, S. L.; Kim, E. M.; Kim, D. W.; Lim, S. T.; Jang, K. Y.; Jeong, Y. Y.; Nah, J. W.; Sohn, M. H. SPION-loaded chitosan−linoleic acid nanoparticles to target hepatocytes. *Int. J. Pharm.* **2009**, *371* (1−2), 163−169.

(192) Velusamy, P.; Chia-Hung, S.; Shritama, A.; Kumar, G. V.; Jeyanthi, V.; Pandian, K. Synthesis of oleic acid coated iron oxide nanoparticles and its role in anti-biofilm activity against clinical isolates of bacterial pathogens. *Journal of the Taiwan Institute of Chemical Engineers* **2016**, *59*, 450−456.

(193) Xiao, L.; Huang, H.; Fan, S.; Zheng, B.; Wu, J.; Zhang, J.; Pi, J.; Xu, J. F. Ferroptosis: A mixed blessing for infectious diseases. *Front Pharmacol* **2022**, *13*, No. 992734.

(194) Paradkar, P. N.; De Domenico, I.; Durchfort, N.; Zohn, I.; Kaplan, J.; Ward, D. M. Iron depletion limits intracellular bacterial growth in macrophages. *Blood, The Journal of the American Society of Hematology* **2008**, *112* (3), 866−874.

(195) Zhang, Y.-M.; Rock, C. O. Membrane lipid homeostasis in bacteria. *Nature Reviews Microbiology* **2008**, *6* (3), 222−233.

(196) Ozdal, M.; Gurkok, S. Recent advances in nanoparticles as antibacterial agent. *ADMET and DMPK* **2018**, *10* (2), 115−129.

(197) Linklater, D. P.; Baulin, V. A.; Le Guével, X.; Fleury, J.-B.; Hanssen, E.; Nguyen, H. P.; Juodkazis, S.; Bryant, G.; Crawford, R.; Stoodley, P. Antibacterial Action of Nanoparticles by Lethal Stretching of Bacterial Cell Membranes. *Advanced Materials* **2020**, *32* (52), No. 2005679, DOI: 10.1002/adma.202005679.

(198) Nosaka, Y.; Nosaka, A. Y. Generation and detection of reactive oxygen species in photocatalysis. *Chem. Rev.* **2017**, *117* (17), 11302−11336.

(199) Vaishampayan, A.; Grohmann, E. Antimicrobials functioning through ros-mediated mechanisms: Current insights. *Microorganisms* **2022**, *10* (1), 61.

(200) Yang, Y.; Wang, C.; Wang, N.; Li, J.; Zhu, Y.; Zai, J.; Fu, J.; Hao, Y. Photogenerated reactive oxygen species and hyperthermia by Cu3SnS4 nanoflakes for advanced photocatalytic and photothermal antibacterial therapy. *J. Nanobiotechnol.* **2022**, *20* (1), 195.

(201) Touati, D. Iron and oxidative stress in bacteria. *Archives of biochemistry and biophysics* **2000**, *373* (1), 1−6.

(202) Seixas, A. F.; Quendera, A. P.; Sousa, J. P.; Silva, A. F.; Arraiano, C. M.; Andrade, J. M. Bacterial response to oxidative stress and RNA oxidation. *Frontiers in Genetics* **2022**, *12*, No. 821535.

(203) Vedernikova, I. Magnetic nanoparticles: Advantages of using, methods for preparation, characterization, application in pharmacy. *Review Journal of Chemistry* **2015**, *5* (3), 256−280.

(204) Anik, M. I.; Mahmud, N.; Masud, A. A.; Khan, M. I.; Islam, M. N.; Uddin, S.; Hossain, M. K. Role of reactive oxygen species in aging and age-related diseases: a review. *ACS Applied Bio Materials* **2022**, *5* (9), 4028−4054.

(205) Canaparo, R.; Foglietta, F.; Limongi, T.; Serpe, L. Biomedical Applications of Reactive Oxygen Species Generation by Metal Nanoparticles. *Materials* **2021**, *14* (1), 1−14.

(206) Deshpande, O. A.; Mohiuddin, S. S. *Biochemistry, Oxidative Phosphorylation*; StatPearls, 2022.

(207) Dunn, J.; Grider, M. H. *Physiology, Adenosine Triphosphate*; StatPearls, 2023.

(208) Tirichen, H.; Yaigoub, H.; Xu, W.; Wu, C.; Li, R.; Li, Y. Mitochondrial Reactive Oxygen Species and Their Contribution in Chronic Kidney Disease Progression Through Oxidative Stress. *Frontiers in Physiology* **2021**, *12*, 398−398.

(209) Zhao, R. Z.; Jiang, S.; Zhang, L.; Yu, Z. B. Mitochondrial electron transport chain, ROS generation and uncoupling (Review). *Int. J. Mol. Med.* **2019**, *44* (1), 3−15.

(210) Zorov, D. B.; Juhaszova, M.; Sollott, S. J. Mitochondrial Reactive Oxygen Species (ROS) and ROS-Induced ROS Release. *Physiol. Rev.* **2014**, *94* (3), 909−909.

(211) Martínez-Reyes, I.; Cuezva, J. M. The H+-ATP synthase: A gate to ROS-mediated cell death or cell survival. *Biochimica et Biophysica Acta (BBA) - Bioenergetics* **2014**, *1837* (7), 1099−1112.

(212) Dissanayake, N. M.; Current, K. M.; Obare, S. O. Mutagenic Effects of Iron Oxide Nanoparticles on Biological Cells. *International Journal of Molecular Sciences* **2015**, *16* (10), 23482−23482.

(213) Ansari, M. O.; Parveen, N.; Ahmad, M. F.; Wani, A. L.; Afrin, S.; Rahman, Y.; Jameel, S.; Khan, Y. A.; Siddique, H. R.; Tabish, M.; Shadab, G. G. H. A. Evaluation of DNA interaction, genotoxicity and oxidative stress induced by iron oxide nanoparticles both in vitro and in vivo: attenuation by thymoquinone. *Scientific Reports* **2019**, *9* (1), 1−14.

(214) Radeloff, K.; Ramos Tirado, M.; Haddad, D.; Breuer, K.; Muller, J.; Hochmuth, S.; Hackenberg, S.; Scherzad, A.; Kleinsasser, N.; Radeloff, A. Superparamagnetic Iron Oxide Particles (VSOPs) Show Genotoxic Effects but No Functional Impact on Human Adipose Tissue-Derived Stromal Cells (ASCs). *Materials* **2021**, *14* (2), 263.

(215) Ren, E.; Zhang, C.; Li, D.; Pang, X.; Liu, G., Leveraging metal oxide nanoparticles for bacteria tracing and eradicating. In *VIEW*; John Wiley and Sons Inc, 2020; Vol. 1.

(216) Huang, Y.; Jiang, J.; Wang, Y.; Chen, J.; Xi, J. Nanozymes as Enzyme Inhibitors. *Int. J. Nanomed.* **2021**, *16*, 1143−1155.

(217) Wang, L.; Hu, C.; Shao, L. The antimicrobial activity of nanoparticles: present situation and prospects for the future. *Int. J. Nanomed.* **2017**, *12*, 1227−1249.

(218) Cha, S.-H.; Hong, J.; McGuffie, M.; Yeom, B.; Vanepps, J. S.; Kotov, N. A. Shape-Dependent Biomimetic Inhibition of Enzyme by Nanoparticles and Their Antibacterial Activity. *ACS Nano* **2015**, *9* (9), 9097−9105.

(219) Gupta, D.; Singh, A.; Khan, A. U. Nanoparticles as Efflux Pump and Biofilm Inhibitor to Rejuvenate Bactericidal Effect of Conventional Antibiotics. *Nanoscale Res. Lett.* **2017**, *12* (1), No. 454, DOI: 10.1186/s11671-017-2222-6.

(220) Hasani, A.; Madhi, M.; Gholizadeh, P.; Shahbazi Mojarrad, J.; Ahangarzadeh Rezaee, M.; Zarrini, G.; Samadi Kafil, H., Metal nanoparticles and consequences on multi-drug resistant bacteria: reviving their role. *SN Applied Sciences* **2019**, *1* (4). DOI: 10.1007/s42452-019-0344-4

(221) Molina-Hernandez, J. B.; Aceto, A.; Bucciarelli, T.; Paludi, D.; Valbonetti, L.; Zilli, K.; Scotti, L.; Chaves-López, C. The membrane depolarization and increase intracellular calcium level produced by silver nanoclusters are responsible for bacterial death. *Sci. Rep.* **2021**, *11* (1), No. 21557.

(222) Fahmy, H. M.; Shekewy, S.; Elhusseiny, F. A.; Elmekawy, A. Enhanced Biocompatibility by Evaluating the Cytotoxic and Genotoxic Effects of Magnetic Iron Oxide Nanoparticles and Chitosan on Hepatocellular Carcinoma Cells (HCC). *Cell Biochem. Biophys.* **2024**, 1−16.

(223) Martin, L.; Lopez, K.; Fritz, S.; Easterling, C. P.; Krawchuck, J. A.; Poerwoprajitno, A. R.; Xu, W. Determination of the optical interference of iron oxide nanoparticles in fluorometric cytotoxicity assays. *Heliyon* **2024**, *10* (3), No. e25378.

(224) Prodan-Bărbulescu, C.; Watz, C.-G.; Moacă, E.-A.; Faur, A.-C.; Dehelean, C.-A.; Faur, F. I.; Grigoriţă, L. O.; Maghiari, A. L.; Tuţac, P.; Duţă, C.; et al. A Preliminary Report Regarding the Morphological Changes of Nano-Enabled Pharmaceutical Formulation on Human Lung Carcinoma Monolayer and 3D Bronchial Microtissue. *Medicina* **2024**, *60* (2), 208.

(225) Antoniou, M.; Melagraki, G.; Lynch, I.; Afantitis, A. In Vitro Toxicological Insights from the Biomedical Applications of Iron Carbide Nanoparticles in Tumor Theranostics: A Systematic Review and Meta-Analysis. *Nanomaterials* **2024**, *14* (9), 734.

(226) Shakil, M. S.; Hasan, M. A.; Sarker, S. R. Iron Oxide Nanoparticles for Breast Cancer Theranostics. *Curr. Drug Metab* **2019**, *20* (6), 446−456.

(227) Daviu, N.; Portilla, Y.; Gomez de Cedron, M.; Ramirez de Molina, A.; Barber, D. F. DMSA-coated IONPs trigger oxidative stress, mitochondrial metabolic reprograming and changes in mitochondrial disposition, hindering cell cycle progression of cancer cells. *Biomaterials* **2024**, *304*, No. 122409.

(228) Majeed, S.; Mohd Rozi, N. A. B.; Danish, M.; Mohamad Ibrahim, M. N.; Joel, E. L. In vitro apoptosis and molecular response of engineered green iron oxide nanoparticles with l-arginine in MDA-MB-231 breast cancer cells. *Journal of Drug Delivery Science and Technology* **2023**, *80*, No. 104185.

(229) Rahman, M. Magnetic resonance imaging and iron-oxide nanoparticles in the era of personalized medicine. *Nanotheranostics* **2023**, *7* (4), 424.

(230) Setia, A.; Mehata, A. K.; Vikas; Malik, A. K.; Viswanadh, M. K.; Muthu, M. S. Theranostic magnetic nanoparticles: Synthesis, properties, toxicity, and emerging trends for biomedical applications. *Journal of Drug Delivery Science and Technology* **2023**, *81*, No. 104295.

(231) Wibowo, N. A.; Kurniawan, C.; Kusumahastuti, D. K.; Setiawan, A.; Suharyadi, E. Potential of Tunneling Magnetoresistance Coupled to Iron Oxide Nanoparticles as a Novel Transducer for Biosensors-on-Chip. *J. Electrochem. Soc.* **2024**, *171* (1), No. 017512.

(232) Falsini, S.; Colzi, I.; Dainelli, M.; Parigi, E.; Salvatici, M. C.; Papini, A.; Talbot, D.; Abou-Hassan, A.; Gonnelli, C.; Ristori, S. Impact of airborne iron oxide nanoparticles on Tillandsia usneoides as a model plant to assess pollution in heavy traffic areas. *Chemosphere* **2024**, *355*, No. 141765.

(233) Arami, H.; Khandhar, A.; Liggitt, D.; Krishnan, K. M. In vivo delivery, pharmacokinetics, biodistribution and toxicity of iron oxide nanoparticles. *Chem. Soc. Rev.* **2015**, *44* (23), 8576−8607.

(234) Qi, X.; Wang, S.; Ma, S.; Han, K.; Li, X. Quantitative prediction of flow dynamics and mechanical retention of surface-altered red blood cells through a splenic slit. *Phys. Fluids* **2021**, *33* (5), No. 051902, DOI: 10.1063/5.0050747.

(235) Ilium, L.; Davis, S.; Wilson, C.; Thomas, N.; Frier, M.; Hardy, J. Blood clearance and organ deposition of intravenously administered colloidal particles. The effects of particle size, nature and shape. *International journal of pharmaceutics* **1982**, *12* (2−3), 135−146.

(236) Patil, U. S.; Adireddy, S.; Jaiswal, A.; Mandava, S.; Lee, B. R.; Chrisey, D. B. In vitro/in vivo toxicity evaluation and quantification of iron oxide nanoparticles. *International journal of molecular sciences* **2015**, *16* (10), 24417−24450.

(237) Abu-Huwaij, R.; Al-Assaf, S. F.; Mousli, F.; Kutkut, M. S.; Al-Bashtawi, A. Perceptive review on properties of iron oxide nanoparticles and their antimicrobial and anticancer activity. *Sys. Rev. Pharm.* **2020**, *11* (8), 418−431.

(238) Dandan Doganci, M.; Doganci, E.; Balci, H.; Cetin, M. Antibacterial and cytotoxic performance of methenamine-based poly (lactic acid)/poly (ethylene glycol)(PLA/PEG) composite films. *J. Appl. Polym. Sci.* **2024**, *141* (21), No. e55412.

(239) Nakipoglu, M.; Tezcaner, A.; Contag, C. H.; Annabi, N.; Ashammakhi, N. Bioadhesives with antimicrobial properties. *Adv. Mater.* **2023**, *35* (49), No. 2300840.

(240) Rehman, A.; Khan, S.; Sun, F.; Peng, Z.; Feng, K.; Wang, N.; Jia, Y.; Pan, Z.; He, S.; Wang, L.; et al. Exploring the nano-wonders: unveiling the role of Nanoparticles in enhancing salinity and drought tolerance in plants. *Frontiers in Plant Science* **2024**, *14*, No. 1324176.

(241) Hamdy, N. M.; Boseila, A. A.; Ramadan, A.; Basalious, E. B. Iron oxide nanoparticles-plant insignia synthesis with favorable biomedical activities and less toxicity, in the "era of the-green": a systematic review. *Pharmaceutics* **2022**, *14* (4), 844.

(242) Raheem, M. A.; Rahim, M. A.; Gul, I.; Zhong, X.; Xiao, C.; Zhang, H.; Wei, J.; He, Q.; Hassan, M.; Zhang, C. Y.; et al. Advances in nanoparticles-based approaches in cancer theranostics. *OpenNano* **2023**, *12*, No. 100152.

(243) Hancharova, M.; Halicka-Stępień, K.; Dupla, A.; Lesiak, A.; Sołoducho, J.; Cabaj, J. Antimicrobial activity of metal-based nanoparticles: a mini-review. *BioMetals* **2024**, *37*, 773.

(244) Aliya, S.; Rethinasabapathy, M.; Yoo, J.; Kim, E.; Chung, J.-Y.; Cha, J.-H.; Huh, Y. S. Phytogenic fabrication of iron oxide nanoparticles and evaluation of their in vitro antibacterial and cytotoxic activity. *Arabian Journal of Chemistry* **2023**, *16* (6), No. 104703.

(245) Tao, Z.; Zhou, Q.; Zheng, T.; Mo, F.; Ouyang, S. Iron oxide nanoparticles in the soil environment: Adsorption, transformation, and environmental risk. *Journal of Hazardous Materials* **2023**, *459*, No. 132107.

(246) Kamble, A. Iron Oxide Nanoparticles: An Alternative against Drug-Resistant Uropathogens. *World J. Pharm. Res.* **2022**, *11* (9), 451−476, DOI: 10.20959/wjpr20229-24659.

(247) Rashki, S.; Asgarpour, K.; Tarrahimofrad, H.; Hashemipour, M.; Ebrahimi, M. S.; Fathizadeh, H.; Khorshidi, A.; Khan, H.; Marzhoseyni, Z.; Salavati-Niasari, M.; et al. Chitosan-based nanoparticles against bacterial infections. *Carbohydr. Polym.* **2021**, *251*, No. 117108.

(248) Fu, P. P.; Xia, Q.; Hwang, H.-M.; Ray, P. C.; Yu, H. Mechanisms of nanotoxicity: generation of reactive oxygen species. *Journal of food and drug analysis* **2014**, *22* (1), 64−75.

(249) Min, Y.; Suminda, G. G. D.; Heo, Y.; Kim, M.; Ghosh, M.; Son, Y.-O. Metal-based nanoparticles and their relevant consequences on cytotoxicity cascade and induced oxidative stress. *Antioxidants* **2023**, *12* (3), 703.

(250) Chen, L.-L.; Fan, Y.-G.; Zhao, L.-X.; Zhang, Q.; Wang, Z.-Y. The metal ion hypothesis of Alzheimer's disease and the anti-neuroinflammatory effect of metal chelators. *Bioorganic Chemistry* **2023**, *131*, No. 106301.

(251) Chen, Y.; Hou, S. Recent progress in the effect of magnetic iron oxide nanoparticles on cells and extracellular vesicles. *Cell Death Discovery* **2023**, *9* (1), 195.

(252) Supardianningsih, S.; Susiani, S.; Nugraha, M. Green Synthesis of ZnO Nanoparticles Using Potato Extracts (Solanum tuberosum) As an Antibacterial Agent in the Active Packaging For Food Products. *KnE Engineering* **2024**, *6* (1), 420−428.

(253) Güell, F.; Galdámez-Martínez, A.; Martínez-Alanis, P. R.; Catto, A. C.; da Silva, L. F.; Mastelaro, V. R.; Santana, G.; Dutt, A. ZnO-based nanomaterials approach for photocatalytic and sensing applications: recent progress and trends. *Materials Advances* **2023**, *4*, 3685.

(254) Zhan, Y.; Hu, H.; Yu, Y.; Chen, C.; Zhang, J.; Jarnda, K. V.; Ding, P. Therapeutic strategies for drug-resistant Pseudomonas aeruginosa: Metal and metal oxide nanoparticles. *J. Biomed. Mater. Res., Part A* **2024**, *112*, 1343.

(255) Kapoor, D. U.; Patel, R. J.; Gaur, M.; Parikh, S.; Prajapati, B. G. Metallic and metal oxide nanoparticles in treating Pseudomonas aeruginosa infections. *Journal of Drug Delivery Science and Technology* **2024**, *91*, No. 105290.

(256) Ali, A.; Bairagi, S.; Ganie, S. A.; Ahmed, S. Polysaccharides and proteins based bionanocomposites as smart packaging materials: From fabrication to food packaging applications a review. *Int. J. Biol. Macromol.* **2023**, *252*, No. 126534.

(257) Tornero-Gutiérrez, F.; Ortiz-Ramírez, J. A.; López-Romero, E.; Cuéllar-Cruz, M. Materials used to prevent adhesion, growth, and biofilm formation of Candida species. *Medical Mycology* **2023**, *61* (7), No. myad065.

(258) Hashim, A. F.; Alghuthaymi, M. A.; Vasil'kov, A. Y.; Abd-Elsalam, K. A. Polymer inorganic nanocomposites: A sustainable antimicrobial agents. *Advances and Applications Through Fungal Nanobiotechnology* **2016**, 265−289.

(259) Al-Hakkani, M. F.; Gouda, G. A.; Hassan, S. H.; Nagiub, A. M. Echinacea purpurea mediated hematite nanoparticles (α-HNPs) biofabrication, characterization, physicochemical properties, and its in-vitro biocompatibility evaluation. *Surfaces and Interfaces* **2021**, *24*, No. 101113.

(260) Ghosh, S.; Singh, B. P.; Webster, T. J., Nanoparticle-impregnated biopolymers as novel antimicrobial nanofilms. In *Biopolymer-based nano films*; Elsevier, 2021; pp 269−309.

(261) Jafarizadeh-Malmiri, H.; Sayyar, Z.; Anarjan, N.; Berenjian, A. *Nanobiotechnology in food: Concepts, applications and perspectives*; Springer, 2019.

(262) Pucci, C.; Degl'Innocenti, A.; Belenli Gumus, M.; Ciofani, G. Superparamagnetic iron oxide nanoparticles for magnetic hyper-thermia: recent advancements, molecular effects, and future directions in the omics era. *Biomaterials Science* **2022**, *10* (9), 2103−2121.

(263) Nabil, G.; Bhise, K.; Sau, S.; Atef, M.; El-Banna, H. A.; Iyer, A. K. Nano-engineered delivery systems for cancer imaging and therapy: Recent advances, future direction and patent evaluation. *Drug Discovery Today* **2019**, *24* (2), 462−491.